



HAL
open science

Spatial structure of natural boxwood and the invasive box tree moth can promote coexistence

Léo Ledru, Jimmy Garnier, Christiane Gallet, Camille Noûs, Sébastien Ibanez

► **To cite this version:**

Léo Ledru, Jimmy Garnier, Christiane Gallet, Camille Noûs, Sébastien Ibanez. Spatial structure of natural boxwood and the invasive box tree moth can promote coexistence. 2020. hal-03012003v1

HAL Id: hal-03012003

<https://hal.science/hal-03012003v1>

Preprint submitted on 18 Nov 2020 (v1), last revised 16 Jun 2021 (v2)

HAL is a multi-disciplinary open access archive for the deposit and dissemination of scientific research documents, whether they are published or not. The documents may come from teaching and research institutions in France or abroad, or from public or private research centers.

L'archive ouverte pluridisciplinaire **HAL**, est destinée au dépôt et à la diffusion de documents scientifiques de niveau recherche, publiés ou non, émanant des établissements d'enseignement et de recherche français ou étrangers, des laboratoires publics ou privés.

Spatial structure of natural boxwood and the invasive box tree moth can promote coexistence.

Léo Ledru¹, Jimmy Garnier², Christiane Gallet¹, Camille Noûs³, Sébastien Ibanez¹

¹Univ. Grenoble Alpes, Univ. Savoie Mont Blanc, CNRS, LECA, 38000 Grenoble, France

²Univ. Savoie Mont Blanc, CNRS, LAMA, 73370 Le Bourget-du-Lac, France

³Laboratory Cogitamus

Addresses for correspondance: LL: leo.ledru@univ-smb.fr, JG: jimmy.garnier@univ-smb.fr, CG: christiane.gallet@univ-smb.fr, CN: camille.nous@cogitamus.fr, SI: sebastien.ibanez@univ-smb.fr,

1 Abstract

2 In the absence of top-down and bottom-up controls, herbivores eventually exhaust their host plants driving them-
3 selves to extinction. Poorly mobile herbivores may nevertheless go extinct only locally; then recolonize intact plant
4 patches elsewhere, leaving time to previously over-exploited patches to regrow. However most herbivores such as
5 winged insects are highly mobile, which may prevent the formation of spatial heterogeneity.

6 We test if long-distance dispersal can preclude coexistence using the invasion of box tree moth (*Cydalima*
7 *perspectalis*) in Europe as a model system. We build a lattice model and estimate the parameters with a combination
8 of field measurements, experimental data and literature sources. Space corresponds either to a realistic boxwood
9 landscape in the Alps, or to theoretical landscapes of various sizes.

10 We find that both species persist under a large range of realistic parameter values, despite a severe reduction
11 in boxwood biomass, with an alternation of outbreaks and near-to-extinction moth densities. Large landscapes
12 are necessary for coexistence, allowing the formation of spatial structure. Low plant regrowth combined with
13 long-distance dispersal could drive moths to extinction, because of resources depletion at the global scale even
14 without a complete synchronization of the local dynamics. The spatial dynamics leads to formation of small plant
15 patches evenly distributed in the landscape, because of a combination of local plant dispersal and global indirect
16 competition between plants through their positive effect on moth population size. Coexistence is favored by such
17 heterogeneous landscapes, because empty patches increase moth mortality during dispersal: the system thus creates
18 its own stability conditions.

19 **Key words:** source-sink dynamics, green world, spatial asynchrony, metacommunity, invasive species

20

Author contributions : CG, SI and JG originally formulated the idea, CG, SI, JG and LL developed methodology, LL conducted fieldwork, SI, JG and LL developed the mathematical model, LL performed the numerical analyses, all authors participated in writing the manuscript.

21 Introduction

22 In general, most herbivores do not polish their resources off because they are top-down controlled by their predators
23 [Hairston et al., 1960] as well as bottom-up limited by the defense compounds and the poor nutritional quality of
24 plants [Polis, 1999]. However, in some cases such top-down and bottom-up mechanisms are insufficient, turning the
25 green world brown. In such cases, it has been suggested that the spatial dynamics of plant-herbivore metacom-
26 munities may favor their coexistence [Wilkinson and Sherratt, 2016]. This hypothesis builds upon long-standing
27 theoretical work which has shown that spatial structure promotes the persistence of otherwise unstable prey-predator
28 systems [Hassell et al., 1991, Comins and Hassell, 1996, Amarasekare, 2008], thanks to local extinctions followed
29 by recolonization, in line with metapopulation and metacommunity dynamics [Hanski and Gilpin, 1997, Holyoak
30 et al., 2005]. These theoretical predictions have received robust empirical support by experiments based on animal
31 prey-predator system [Taylor, 1991], as protists [Holyoak and Lawler, 1996, Fox et al., 2017] and field studies with
32 arthropods [Nachman, 1988, Winder et al., 2001].

33 However, there is little evidence showing that the spatial dynamics resulting from interactions between plants
34 and herbivores leads to a green world - or at least to a multi-coloured world with green and brown patches. Many
35 herbivorous insect populations persist thanks to metapopulation dynamics [Tschardt and Brandl, 2004], but this
36 is generally due to other mechanisms than the depletion of their plant resources. For instance, local extinctions
37 can depend on patch size [Eber and Brandl, 1996], on the fluctuation of plant resources (but for other reasons than
38 the herbivore itself [Halley and Dempster, 1996]), or on a combination of ecological succession and catastrophic
39 events [Stelter et al., 1997]. In the well studied ragwort / cinnabar moth system, the moth can go locally extinct
40 following defoliation, but plant patches persist [Myers and Campbell, 1976, Myers, 1976]. Although cinnabar moths
41 contribute to local plant extinction, local plant persistence ultimately depends on habitat suitability, which leads to
42 a source-sink dynamics rather than to a classical metapopulation scenario [van der Meijden and van der Veen-van,
43 1997, Van der Meijden, 1979]. Moreover, the high dispersal ability of cinnabar moths prevents asynchronous local
44 dynamics for the moth, which rules out a metapopulation model of coexistence [Harrison et al., 1995, van der Meijden
45 and van der Veen-van, 1997]. As far as we know, the only documented plant-herbivore system where the plant
46 goes locally extinct due to over-exploitation comprises the Apiaceae *Aciphylla dieffenbachii* and the monophagous
47 weevil *Hadramphus spinipennis*, two species endemic to the Chatham Islands (New Zealand). Increased local weevil
48 densities are associated with local plant extinction [Schöps, 2002], and numerical simulations have shown that spatial
49 structure allows the persistence of the system, provided that the dispersal distance of the herbivore is intermediate
50 [Johst and Schöps, 2003]. However, the ecological conditions which promote the persistence of this particular study
51 system may not hold for other plant-herbivore interactions. In particular, the weevil *H. spinipennis* is wingless and
52 of a large size, which considerably reduces its dispersal ability either by itself, by wind or by birds. In contrast, many
53 insects can disperse at long distances [Wilson and Thomas, 2002, Gillespie et al., 2012]. Long-distance dispersal
54 can promote metapopulation persistence, except when strong density dependence triggers local extinctions [Johst
55 et al., 2002]. In that case, long-distance dispersal events synchronize local extinctions which eventually lead to
56 the extinction of the whole metapopulation [Palmqvist and Lundberg, 1998, Johst et al., 2002]. In plant-herbivore
57 metacommunities, strong density dependence occurs when herbivores overexploit their host down to local extinction.

58 In order to test if plant-herbivore metacommunities can persist despite high abilities of herbivores to disperse,

59 we study the system formed by the common European boxwood *Buxus sempervirens* and the invasive box tree
60 moth (*Cydalima perspectalis*) in Europe. The moth first arrived in Germany in 2006/2007 [Van der Straten and
61 Muus, 2010] via the boxwood trade from Asia [Kenis et al., 2013, Van der Straten and Muus, 2010, Bras et al.,
62 2019]. It is currently quickly spreading throughout Europe [Blackburn et al., 2011], which suggests human and/or
63 natural long-distance dispersal. On the base of its climate envelope, the moth will likely invade most of Europe
64 in the following years [Nacambo et al., 2014], with potentially major ecosystemic consequences [Mitchell et al.,
65 2018]. Defoliation caused by the moth can lead to the death of the boxwood, especially when the bark is also
66 consumed [Kenis et al., 2013]. After total defoliation, boxwood can either grow back or wither completely, if the
67 defoliation becomes too recurrent [Kenis et al., 2013]. The local extinction of boxwood has already been observed in
68 the Nature Reserve of Grenzach-Whylen in Germany [Kenis et al., 2013]. In the meantime, the moth goes extinct
69 locally after total defoliation of boxwood stand, even if it grows back several years after the moth outbreak. Within
70 its area of origin, the moth is regulated by its natural enemies [Wan et al., 2014] and no local extinction of either
71 plant and insect species is observed, but potential european natural enemies do not significantly alter the invasive
72 moth dynamics [Kenis et al., 2013, Leuthardt and Baur, 2013]. Moreover, although box trees contain highly toxic
73 alkaloids [Ahmed et al., 1988, Loru et al., 2000, Devkota et al., 2008], the moth larvae can sequester them in their
74 body [Leuthardt et al., 2013], which may rule out bottom-up control. In contrast, in the ragwort / cinnabar and
75 Apiaceae / weevil systems mentioned earlier, both insects are native and may therefore be top-down controlled by
76 local natural enemies. Given that both top-down and bottom-up controls are disabled in the case of the invasive
77 boxwood moth, will the European boxwood stands remain green?

78 Metacommunity dynamics with local moth extinctions followed by recolonization may be an alternative mech-
79 anism to top-down and bottom-up control favouring coexistence in Europe. In the particular context of biological
80 invasions, spatial effects have not been widely addressed [Melbourne et al., 2007], although they may favour coex-
81 istence. The metacommunity mechanism requires spatial heterogeneity among local communities, which is likely
82 because boxwood has a fairly fragmented distribution in Europe, and because the box tree moth was not simultane-
83 ously introduced in every patch. As long as the invasion does not start simultaneously in all stands, the moth may
84 disperse from its current totally defoliated stand to a green intact stand. The defoliated stands may then grow back
85 and be recolonised lately. Thus, despite local extinctions and recolonizations, local fluctuations may be averaged on
86 a large spatial scale, leading to a global stationary regime which has been called 'statistical stability' [De Roos et al.,
87 1991, Holyoak et al., 2005, Amarasekare, 2008]. However, unlike the wingless weevil *H. spinipennis*, *C. perspectalis*
88 is highly mobile, because it can fly or it can be transported by exogenous factors (wind, human activities) [Bras
89 et al., 2019]. Its high mobility may prevent spatial heterogeneity and therefore precludes coexistence by spatial
90 effects [Johst et al., 2002, Johst and Schöps, 2003]. Thus at large spatial scale, three ecological scenarios are likely
91 to occur. First, the moth might very quickly overexploit its host, causing it own extinction but not the one of its
92 host, which in turn slowly grows back. Second, the moth might persist long enough to exhaust its host, leading
93 to the extinction of both species. Third, coexistence might result from the balance between local moth extinctions
94 and recolonizations, without complete resource depletion. Our study focuses on the conditions which favor such
95 coexistence, based on the following hypotheses :

- 96 1. Long-term coexistence of boxwood and moth is possible at the landscape scale through spatial stabilizing
97 effects (1a). Those effects rely on asynchronous local dynamics (1b).

- 98 2. Despite cycles of local extinctions and recolonizations, the coexistence regime is stationary at the regional
99 scale, which corresponds to statistical stability.
- 100 3. Dispersal is double-edged : very limited dispersal might prevent the colonization of green patches (3a), whereas
101 long-distance dispersal may synchronize local dynamics (3b).
- 102 4. The coexistence regime depends on the landscape characteristics, in particular the landscape size and the
103 proportion of boxwood patches in the landscape. First, larger landscapes favor coexistence (4a). Secondly,
104 the effect of the proportion of boxwood patches is uncertain, since it provides more resources to the moth,
105 but also favors outbreaks and resource depletion (4b).

106 In order to address these four hypotheses, we develop a population model dynamics for the boxwood and moth
107 system. First, a local model reproduces the local invasion dynamics, which invariably leads to moth extinction
108 in the field. Then, a spatially explicit model simulates the dynamics of the moth in a landscape. Our model is
109 calibrated from the literature, *in situ* measures, and through mesocosm experimentation.

110 Study system & theoretical model description

111 Species involved : boxwood and box tree moth

112 The box tree moth, *Cydalima perspectalis*, is an herbivorous lepidoptera belonging to the Crambidae family [Mally
113 and Nuss, 2010]. Five to seven stages of development are necessary to the larvae to become nymphs for about ten
114 days before emerging as moths [Kawazu et al., 2010]. During the winter, the larvae are at the beginning of their
115 development in stages two or three and form cocoons to enter in diapause [Nacambo et al., 2014]. The moths live
116 for two weeks during which they reproduce and lay eggs on boxwood leaves. The moth has a high fecundity rate,
117 with between 300 and 400 eggs laid per female [Kawazu et al., 2010, Wan et al., 2014]. In Asia, two to five life
118 cycles are possible per year, with a break during the winter when the caterpillars are dormant [Maruyama et al.,
119 1987, 1991]. In its invasion range, the moth completes from 2 (in the north) to 4 (in the south) generations per year
120 [Nacambo et al., 2014, Göttig, 2017]. The mean intrinsic dispersal distance of moths has been estimated around
121 ten kilometers per year [Van der Straten and Muus, 2010].

122 The moth exhibits no preference for any particular boxwood species [Leuthardt and Baur, 2013], so the common
123 European boxwood *Buxus sempervirens* is widely consumed, as well as Caucasus boxwood *Buxus colchica*, and even
124 the rarer European species *Buxus balearica* [Kenis et al., 2013]. These natural boxwood stands, which have already
125 undergone a major decline over the last millennia [Di Domenico et al., 2012], are now subject to this additional
126 threat. In Asia, *C.perspectalis* also consumes other species, including holly (*Ilex purpurea*), charcoal (*Euonymus*
127 *japonicus*, and *E.alatus*). Fortunately this is not currently the case in Europe [Göttig, 2017]. Despite natural
128 regulation by native predators and parasites, this moth remains a threat to ornamental boxwood in Asia, where
129 its potential targets are protected by insecticides [Wan et al., 2014]. Instead, in Europe *Bacillus thuringiensis* is
130 commonly used as a sustainable control method. However, its efficiency is offset by its low persistence; current
131 efforts are being made to develop more long-term treatments. Biological control solutions are also being explored,
132 such as the use of nematodes [Göttig and Herz, 2018] and parasites from the genus *Trichogramma* [Göttig and Herz,
133 2016]. Efforts are also being made to seek out predators and parasites from the box tree moth's area of origin that

134 might act in areas of invasion [Göttig, 2017]. The use of pheromone traps is widespread, both for monitoring and
 135 control [Santi et al., 2015, Göttig and Herz, 2017], but their effectiveness appears to be insufficient at a large scale.
 136 Even if effective control for ornamental boxwood could be introduced, natural boxwood and associated ecosystems
 137 will likely suffer dramatically from the *C.perspectalis* invasion.

138 Boxwood has a fairly heterogeneous distribution in Europe that consists mainly of small and fragmented stands,
 139 but some large areas of continuous boxwood occur in the French Pyrenees, the Pre-Alps and the Jura [Di Domenico
 140 et al., 2012]. It is a long-lived, slow-growing shrub that thrives on calcareous substrate. It can tolerate a wide
 141 gradient of light incidence, and can therefore be found in a range of plant communities, from canopy areas in heaths
 142 to under cover in forests [Di Domenico et al., 2012]. It can play an important role in structuring ecosystems, by
 143 trapping sediment and storing water. It also influences the establishment and survival of tree species in wood-
 144 land succession [Mitchell et al., 2018]. A total of 286 species are associated with the shrub, including 43 fungi that
 145 are exclusively observed on boxwood [Mitchell et al., 2018]. However, boxwood is scarcely predated by native species.

146

147 Demographic model on the local scale

148 Our model projects the population size m of Box Tree Moths (BTM) and the population density of Box Trees
 149 (BT), which are separated in two variables : leaf density l and wood density w , from moth generation n to $n + 1$.
 150 This time representation is used to avoid the problem of multiple generations per year and its variation with space
 151 location. However, we are able to project the population of BTM and BT from year to year if we know the number
 152 of generations per year in each specific location. We write

$$\left\{ \begin{array}{l} l_{n+1} = S_l(\mu_n) F_l(l_n) l_n + r_0 w_n \\ w_{n+1} = S_w(\mu_n, \rho_n) F_w(w_n, \rho_n) w_n \\ m_{n+1} = S_m(\mu_n) F_m m_n \end{array} \right. \quad (1)$$

153 to indicate that during the projection interval, BT and BTM grow and reproduce (F), and survive (S). The BT
 154 reproduction functions were constructed using a Ricker model, which includes the intrinsic population growth rates
 155 r_f, r_w and the carrying capacity of the environment L_{max}, W_{max} , while the BTM reproduction function is linear
 156 and only includes the fecundity of adults f and their survival s . The survival of the species is determined by the
 157 consumption of leaves and bark by the BTM as well as the intraspecific competition for the resource faced by
 158 BTM. The survival and reproduction functions F and S depend on both the current population l, w, m , and the
 159 environmental descriptors μ and ρ .

160 **Environmental descriptors.** The environmental quality is described using two descriptors μ and ρ defined
 161 by ratios of population densities:

$$\mu_n = \frac{f m_n \alpha}{l_n} \quad \text{and} \quad \rho_n = \frac{l_n}{w_n}$$

162 The ratio μ corresponds to the ratio between the number of leaves needed by all the larvae to fulfil their cycle and
 163 the number of available leaves (α is the amount of leaves needed per larva). The number of larvae depends on the
 164 number of moths (m_n) through its product by the moth fecundity (f). And each larva needs α leaves to complete

165 its cycle. The ratio μ thus quantifies the pressure for the resource, which plays a direct role in the intensity of
 166 consumption of leaves and wood, and therefore the survival of the larvae.
 167 The ratio ρ is the quantity of leaves per unit of wood. This represents the level of boxwood defoliation, which has
 168 an impact on the growth of the wood.

169 **Reproduction.** The increase in foliage biomass is the result of two processes: the growth of leaves F_l , which
 170 depends on the current foliage (Figure 1a), and the production r_0 of new shoots by the wood after defoliation
 171 (Figure 1b). Without herbivory, the growth of leaves is limited only by senescence and carrying capacity L_{max} .
 172 Thus, growth F_l is represented by a Ricker model in the following form

$$F_l(l) = \exp\left(r_f\left(1 - \frac{l}{L_{max}}\right)\right)$$

173 where r_f is the intrinsic growth rate of the leaves.
 174 The wood growth function F_w (Figure 1c) is constructed using a Ricker model. Positive growth ($r_w > 0$) is
 175 constrained by carrying capacity. Negative growth ($r_w \leq 0$) occurs after an important defoliation because branches
 176 or even a proportion of trunk can die after defoliation. For each projection interval n , the intrinsic growth rate of
 177 the wood $r_w(\rho_n)$ is defined as the balance between the production of new wood b_w , which critically depends on the
 178 density of leaves per unit of wood ρ_n , and the mortality induced by severe defoliation d_w .

$$179 \quad F_w(w, \rho) = \begin{cases} \exp(r_w(\rho)(1 - \frac{w}{w_{max}})) & \text{if } r_w(\rho) > 0 \\ \exp(r_w(\rho)) & \text{if } r_w(\rho) \leq 0 \end{cases} \quad \text{with } r_w(\rho) = b_w(\rho) - d_w(\rho)$$

180 When the density of leaves is large ($\rho \gg 1$), the BT is healthy and its production of wood reaches a maximum
 181 $r_{w,max}$. Conversely, when the density of leaves per unit of wood collapses due to severe defoliation, the production
 182 of wood is low while the mortality increases until a maximum $-r_{w,min} < 0$ which forces the growth rate to be
 183 negative. The production function b_w and the mortality function d_w takes the following form :

$$b_w(\rho) = \frac{\rho^{\beta_r}}{\rho^{\beta_r} + \theta_r^{\beta_r}} r_{w,max} \quad d_w(\rho) = (1 - d^{\frac{1}{\rho}}) r_{w,min} \quad (2)$$

184 where β_r , θ_r and d are shape parameters (see Table 1).

185
 186 The reproduction rate of BTM (Figure 1d) does not suffer from density dependence and is equal to the product of
 187 adult fecundity f and adult survival s

$$F_m = f s$$

188 **Survival.** The leaves may die by senescence at rate v , or be consumed by BTM at a rate which increases with
 189 the pressure of BTM on BT, μ , (Figure 1e). In the absence of BTM, 0% of leaves are consumed, while if BTM have
 190 saturated the environment, 100% of the leaves are consumed. Thus the survival function of the leaves is defined by

$$S_l(\mu) = v(\sigma_l^\mu) \quad (3)$$

191 where σ_l is a shape parameter (see Table 1).

192

193 The wood can suffer from both defoliation (Figure 1c), which decreases its intrinsic growth rate, and from the
194 consumption of bark by the BTM (Figure 1f).

195 The wood mortality due to consumption increases with both the BTM pressure, μ and the BT health ρ . More
196 precisely, the wood mortality saturates to d_{max} when the foliage is abundant (large ratio $\rho \geq 1/3$). However, when
197 the foliage is small (low ratio $\rho \leq 1/3$), the bark consumption occurs while the superficial woods is available. Thus
198 recently defoliated boxwood with small bark coverage (ρ close to 0) cannot be consumed by the larvae.

$$S_w(\mu, \rho) = 1 - \frac{\mu^{\beta_s}}{\mu^{\beta_s} + \theta_s^{\beta_s}} D_{max}(\rho) \quad (4)$$

199 where β_s and θ_s are shape parameters and D_{max} is the maximal mortality rate which grows linearly with ρ until a
200 threshold $1/3$, at which point it saturates to its critical value d_{max} .

$$D_{max}(\rho) = \begin{cases} 3d_{max} \rho & \text{if } \rho < 1/3 \\ d_{max} & \text{if } \rho \geq 1/3 \end{cases} \quad (5)$$

201 This step function takes into account that the consumption of superficial wood depends on the presence of available
202 softwood, and thus a certain amount of foliage. The threshold value $1/3$ for BTM pressure ρ corresponds to the
203 approximate ratio when there is as much foliage as wood, the density of the wood being three times greater.

204

205 Survival of BTM during the larval stage depends mainly on the amount of available resource per larva μ . If the larva
206 has enough available resource to complete its six stages, it will evolve into a moth, while a lack of resource during its
207 growth will cause its death. The survival rate also takes into account intraspecific competition for resource caused
208 by interference between the larvae. The survival function is defined using a shape parameter σ_m as

$$S_m(\mu) = \begin{cases} S_{m,max} \left(1 - (\sigma_m)^{\frac{1}{\mu}}\right) & \text{if } \mu < 2 \\ 0 & \text{if } \mu > 2 \end{cases} \quad (6)$$

209 The threshold $\mu = 2$ fits a given situation that occurs when there is a shortage of resource for the larvae, even if
210 some larvae die during their evolution.

211 Spatially explicit model

212 The local model allows us to describe the interaction between BTM and its host BT at a small homogeneous spatial
213 scale. Next, we build a cellular automaton in order to investigate the BTM invasion over a regional heterogeneous
214 landscape. From field observations provided by the National Alpine Botanical Conservatory, we obtain a map of
215 the French Alps composed of 570 by 351 cells of 29 hectares each (about 58 000km², see Online Resource 1 in
216 Supporting Information). It should be noted that these data focus on natural boxwood and neglect the presence of
217 ornamental boxwood in urban areas. We focus on the French Alps because detailed botanical data are available,

218 but in theory our model could be extended to the whole area of invasion. Green cells correspond to areas with
 219 BT, grey cells correspond to areas without BT, while blue cells represent urban areas. We use the basemap from
 220 OpenStreetMap based in Qgis[®]. In each cell with BT, BTM can mate and lay eggs according to the local model,
 221 while in cells without BT, BTM cannot become established. After the reproduction phase, BTM moths disperse
 222 over the landscape to find new areas to breed and lay eggs. BT can also disperse over the landscape to recolonise
 223 extinct areas. Simulations are initialized with a single moth invading a patch chosen at random, and carried out on
 224 a maximum of 1000 iterations if no specifications are given.

225 **Dispersal phase of BTM.** A BTM dispersal event includes two stages: (1) emigrating from birth areas, and
 226 (2) searching for new areas (exploration) and settling to breed. Field observations suggest that the exploration
 227 phase is stochastic, composed of frequent short-distance dispersal by adult flight, and rare long-distance dispersal
 228 by anthropogenic action (boxwood trade) or long flight. *In situ* experimentation using a flight carousel has provided
 229 a mean dispersal distance per individual of 13km (Bras et al., personal communication), which is in accordance
 230 with the 10km dispersal distance observed by Van der Straten and Muus [2010]. Bras et al. have also observed rare
 231 long-distance flights in their experiments, which may correspond to long-distance dispersal events that we model
 232 using a fat-tailed dispersal kernel. To this end, we use an exponential power distribution from Klein et al. [2006]
 233 which makes it possible to compare different shape of distribution tails while maintaining a fixed average dispersal
 234 distance. For ecologically realistic calibration the tail shape parameter is 0.5 (i.e fat-tailed dispersal kernel) and
 235 the average dispersal distance is 25 cells (i.e ≈ 13 km). In addition, to save computation time, we assume that
 236 BTM disperses as a swarm of 1000 individuals. This group dispersal may occur because BTM can be attracted by
 237 volatile boxwood compounds or avoid geographical barriers, or are influenced by weather conditions. Thus, during
 238 the searching and settling phase, each group of BTM settles in an area located at a random distance drawn in the
 239 exponential power distribution and chosen with a random turning angle run in a uniform distribution over $(0, 2\pi)$.
 240 The emigration rate for each location depends on the pressure for resource μ at the birth location. As long as
 241 pressure remains low, the moths have the possibility to find leaves to oviposit in their birth patch and thus dispersal
 242 is weak. When the resource pressure increases, there is not enough boxwood available for laying eggs and adults
 243 will disperse massively to another patch in search for resource. Such resource-dependent dispersal has also been
 244 modelled by the study of Johst and Schöps [2003]. The migration rate M_m of BTM depends on μ as follows

$$M_m(\mu) = (1 - \delta^\mu)M_{m,max} \quad (7)$$

245 where the maximal dispersal rate $M_{m,max}$ takes into account mortality during the dispersal. Thus the number of
 246 dispersal events at each location is given by $\frac{M_m(\mu)m}{1000}$.

247

248 **Dispersal of BT.** Dispersal events for BT include (1) creation of seeds and (2) dispersal of seeds to surrounding
 249 areas by wind and birds. We assume that BT dispersal is very low and occurs only if the boxwood is in fairly good
 250 condition, meaning that it has sufficient foliage. Thus the dispersal rate of BT depends on the foliage ratio per BT,

251 ρ

$$M_w(\rho) = \begin{cases} (\omega_w)^{1/\rho} M_{w,max} & \text{if } \rho > 1/3 \\ 0 & \text{otherwise} \end{cases} \quad (8)$$

252 As such, the initial density of wood in a newly dispersed seedling depends on the parent patch density. Foliage
253 is produced in the next generation after recolonization through the production of leaves by the wood ($r_0 w_n$ in
254 equation (1)). We assume that seeds from a location are transported randomly only in the 8 surrounding cells that
255 has previously contained BT. We only make it possible for an extinct area to be recolonized by surrounding BT,
256 and we make it impossible for BT to colonize new areas.

257 Theoretical landscape

258 To investigate the effect of the spatial structure we run our model on a square landscape with various initial size
259 and proportion of boxwood patches. For each landscape, we also calculate an aggregation index by counting the
260 number of pairs (adjacent boxwood patches) in the landscape and dividing it by the maximum number of possible
261 pairs: $2n - |2\sqrt{n}|$, where n is the proportion of boxwood cells [Harary and Harborth, 1976]. For each landscape size
262 and boxwood proportion, we randomly generate 1000 landscapes with possibly different aggregation indices. The
263 final aggregation index equals the difference between the index of the landscape of interest and the average index
264 of the randomly generated landscapes.

265 Cluster detection is done using the function Matlab[®] FINDCLU from the File Exchange of MathWorks. To fit the
266 power-law to the cluster-size distribution, we define size-classes of five cells and evaluate the number of clusters in
267 each class.

268 Parameter estimation

269 We use three measurement methods to calibrate the model parameters: 1) field measurements, 2) literature review,
270 3) mesocosm experiment. Some unmeasured parameters are estimated in order to obtain coherence between the
271 simulations, the observations in the field, and the literature.

272

273 Fecundity parameter f

274 Females lay about 300-400 eggs at a time [Kawazu et al., 2010, Wan et al., 2014]. However, the model does not
275 separate males from females, and survival is calculated for caterpillars but not for eggs. The sex ratio seems signif-
276 icantly skewed in favor of males, with only $43\% \pm 10\%$ of the population being females, according to Götting [2017].
277 The hatchability rate is about $79.7\% \pm 2\%$ according to Kawazu et al. [2010]. The fertility parameter is therefore
278 estimated with these bibliographic data using the value: $f = \text{number of eggs} * \text{percentage of female} * \text{hatchability}$
279 $\text{rate} = 120$, with a range from 0 (i.e effects of oophagus predators and parasites) to 300.

280

281 Box tree moth survival function and wood consumption function

282 To determine the survival function according to the pressure for resource μ , the maximum caterpillar survival
283 $S_{m,max}$ is estimated using the bibliographic data. Through lab experimentation, Kawazu et al. [2010] have obtained
284 the following parameters: a larvae survival rate of 78%, a pupation rate of 70%, and an emergence rate of 89%.

285 Thereby, we estimate $S_{m,max} = 49\%$ which seems appropriate because in this laboratory experiment the caterpillars
286 have not undergone any starvation stress. However, for this function, the second parameter σ_m also has to be set;
287 this parameter is difficult to measure because it has no ecological interpretation. Nonetheless, it is possible to obtain
288 different survival values for different μ in order to make a qualitative adjustment of the survival curve. To do this,
289 we performed a mesocosm experiment from April 4 to late May 2018, located on the University of Savoie Mont Blanc
290 campus, in an isolated grassy area (45°38'30.0"N 5°52'02.7"E). Climatic conditions were close to those of nearby
291 natural boxwood stands. We created a pressure range for the resource by placing varying numbers of caterpillars
292 on the box trees. The range included seven μ values, with four replicas for each and four controls. Each of the 32
293 boxwood were isolated in cages of 1m³ covered by mesh (insect proof netting PE 22:30, 920x920; DIATEX, Saint
294 Genis Laval, France) to prevent movement of the larvae between the boxwood. All of the boxwood shrubs came
295 from the same supplier and had received no chemical treatment. They measured 30 cm high and were cultivated in
296 1 liter pots.

297 To establish the pressure range, we estimate the parameter α corresponding to the amount of leaves needed by a
298 moth for its larval cycle, for each value of μ . [Slansky Jr and Scriber \[1982\]](#) provide a mean value of ingested food
299 conversion efficiency (ECI) of 20% for herbivorous Lepidoptera. Knowing that $ECI = B/I$ with B being gained mass
300 and I being ingested food, we obtain I through measurements of dry caterpillar masses performed by T. Defferier and
301 E. Tabone from the National Research Institute for Agriculture, Food and Environment (INRAE). Then, using the
302 average dry mass of the leaves, we convert I into the number of leaves ($I = 25$ leaves). Finally, the number of leaves
303 was counted for each boxwood. Therefore, the value of simulated μ could be determined when a certain number
304 of caterpillars were deposited on a particular box tree. The range used was: $\mu = [2; 1; 0.75; 0.5; 0.25; 0.13; 0.07]$ (see
305 Online Resource 2).

306 This experimentation also make it possible to calibrate the leaf consumption function. At the end of the experiment,
307 when the surviving larvae had reached the adult stage, we counted the living leaves on the boxwood in order to
308 obtain the percentage of leaves that were consumed. The insect-free controls allowed us to distinguish between mor-
309 tality caused by caterpillars and mortality due to the environment. The qualitative calibration of the consumption
310 curve is thus established using the consumption percentages as a function of μ .

311

312 **Wood mortality function**

313 Boxwood mortality by senescence is very low and some boxwood may be over 600 years old. However, box trees
314 attacked by 2 or 3 successive generations may have high probabilities of death [[Kenis et al., 2013](#)]. It is necessary to
315 calibrate mortality due to consumption of superficial wood by the late larva stage caterpillars, D_{max} , and notably
316 the parameter d_{max} . Two wild boxwood locations are used to make *in situ* measurements. These boxwood areas are
317 located on the eastern slope of the Epine massif in Savoie (45°38'23.7"N 5°50'43.6"E and 45°41'33.2"N 5°50'56.2"E)
318 at an altitude of 500 and 630 meters, respectively. This massif has large stands of wild boxwood under trees in
319 limestone soil. The peak invasion and defoliation of the boxwood occurred in July and August 2016, and mortality
320 measurements were made in March 2017.

321 Mortality is assessed in terms of biomass rather than in terms of individuals, using the following procedure: the
322 percentage of living biomass is measured on completely defoliated boxwood according to the level of branching
323 (trunk or branch). For the trunk, the percentage of the total height of the boxwood with shoots (h) is measured,

324 and for branches the percentage of branches with shoots (r), is measured. The mortality d_{max} is estimated by:
325 $d_{max} = 1 - \frac{h+r}{2}$. The measurements made on 101 boxwoods give $d_{max} = 0.74$.

326

327 **Shoot production parameter**

328 The production of shoots from wood, r_0 , is measured by estimating the biomass of shoots produced by wood whose
329 1) live biomass is estimated and 2) defoliation date is known. First, the average mass of a shoot is measured from
330 250 shoots. Then, for each measured boxwood ($N = 49$), the living wood biomass is estimated by considering the
331 trunk as a cone whose volume could be calculated using its circumference and height, with the same calculations
332 made for the branches. This volume, multiply by the density of the wood ($0.95g.cm^{-3}$), gave the biomass of living
333 wood. We count number of shoots and are able to obtain the biomass of the shoots. Thus, $r_0 = \frac{shoots\ biomass}{wood\ biomass} * \frac{1}{time}$
334 with $time$ being the number of generations since defoliation.

335 For the 49 boxwoods measured, the amount of new growth varies from 1 to 154 with an average of 45, giving
336 $r_0 = 5 * 10^{-5}$.

337

338 **Wood growth function**

339 Calibration of the growth function from empirical measurements is performed only for the maximum growth value
340 $r_{w,max}$. For this, a method of dendrometry is used. We have cut some trunk sections with different circumferences
341 (1.5, 2.4, 3.8, 4, 4.9, 5.6, 7.8 centimeters), and we have counted their rings number (respectively 11, 15, 20, 25, 32,
342 36, 50). We assume that boxwood is a cone whose increase in height is proportional to its increase in width, and
343 its growth is proportional to its density. Thus we can infer the maximal growth rate per year $r_{w,max} = 0.134$ using
344 a linear regression. Thus, the growth per generation in the case of two generations of moth per year is 0.067. We
345 obtain a low estimate because we consider that the growth of individuals is already occurring, but not the formation
346 of new individuals while $r_{w,max}$ takes it into account. From the simulation of the model in the absence of herbivory,
347 and this experimental value, $r_{w,max} = 0.3$ is used to model a consistent boxwood growth rate.

348 **Experimental results**

349 Two functions are calibrated according to the experiment: a function for the consumption of leaves by caterpillars
350 (Figure 2a) and a function for caterpillar survival (Figure 2b). These two functions are dependent on competition
351 for the resource through μ . For the leaf consumption function, we quantify the mortality due to senescence from
352 the difference between the average number of initial and final leaves in absence of moth pressure ($\mu = 0$), and then
353 deduct that from the initial number of leaves for each boxwood. This allows one to express in the results only the
354 proportion of dead leaves due to the action of the caterpillars, but it implies the hypothesis that all boxwood suffer
355 about the same mortality due to senescence. Therefore, the control box trees had 100% of non-consumed leaves.

356 Leaf consumption reaches a threshold for $\mu = 1$, i.e. when resources present and resources needed are similar, above
357 which the entire resource is consumed. Similarly, it is the threshold at which survival reaches its lowest value and
358 nearly stagnates. The results presented here show survival until the pupal stage, but at the end of the experiment
359 no moths emerge in the box trees when $\mu = 2$, which is why the survival function is set to 0 for $\mu = 2$.

360 These results are remarkable because they are similar to those expected with a defoliation saturation threshold at
361 $\mu = 1$ and a drastic drop in moth survival. They support our model and minimise the uncertainties that we may
362 have on other parameters.

364 Local model

365 Field observations show that when the box tree moth colonizes a patch, its population explodes within a few
 366 generations, eventually reaching a peak of density which results in total defoliation of the boxwood stand. At this
 367 point no more resources are available and the box tree moth disappears from this patch. We estimate the remaining
 368 model parameters in order to reproduce this qualitative behaviour, and to achieve plausible quantitative outputs
 369 (these parameters are referred as "estimate" in Table 1).

370 Figure 3 simulates the invasion dynamics as expected. The boxwood (leaf and wood) starts at its carrying
 371 capacity, which is calculated from a simulation without moths, and a single box tree moth is added to the patch.
 372 Within six generations, the moth population reaches its peak abundance. During the 7th generation, the ratio μ
 373 between the number of leaves needed by the larvae and the available leaves becomes too large and the survival of
 374 the moth drops to 0. At this point, the effect on boxwood density is maximal. Leaves are entirely consumed by the
 375 early larval stages, which cannot reach their final stages and die from starvation. Still, leaf density does not reach
 376 0 because new leaves grow from wood (at rate r_0w). In a more ecologically accurate representation, the density
 377 of the leaves would drop to 0 and then new leaves would only be produced in the next generation, but this would
 378 not change the model's outputs. Moreover, this phenomenon is implicitly present since all of the moths in the 7th
 379 generations die from starvation and cannot consume the new leaves produced, so it is comparable to a production of
 380 new leaves during the next generation. In natural conditions, however, intact boxwood patches will be more likely
 381 invaded by a larger number of moths. In the spatial version of the model, dispersal events occur with groups of
 382 1000 individuals due to volatile compounds or other exogeneous attractors, and in that case the peak is reached as
 383 early as the 4th generation, and the moth population crashes at the 5th generation.

384 Although the moth population collapses for realistic parameter values, with different parameters the model
 385 allows a positive equilibrium for the three state variables, i.e. the coexistence of moth and boxwood (wood and
 386 leaves). We therefore built map of the final model state in function of moth fecundity and moth survival, two
 387 key parameters which may vary during the course of the outbreak in Europe. The accommodation of native
 388 predators and parasites could indeed reduce the survival rate of caterpillars, and moth fecundity could be reduced
 389 by oophagous insects. The final state map (Online Resource 3) clearly shows that coexistence is only possible in
 390 a very narrow range of parameters values, which are far from the actual measured values. Two connected patches
 391 instead of one can sometimes be enough to favour coexistence in plant-insect interactions [Kang and Armbruster,
 392 2011], but simulations conducted on a two-patch model show only a slight expansion of the coexistence area, which
 393 is far from sufficient to lead to coexistence with realistic parameters (Online Resource 3).

394 Modelling results and discussion

395 Results for hypothesis 1

396 Using a spatially explicit model, including local population dynamics and short to long range dispersal events,
 397 we show that coexistence of the moth/boxwood system occurs across a wide range of parameters. At a regional

398 scale, dispersal allows box tree moth persistence in a cycle outbreak dynamic [Berryman, 1987], through recurrent
399 recolonization of patches that have been previously defoliated and which have had time to recover. The spatial
400 structure therefore allows coexistence, in line with hypothesis 1a. The coexistence mechanism is similar to the
401 rock-paper-scissors game with the corresponding states: patches of defoliated box tree, patches of box tree with
402 foliage and patches of box tree invaded by the moth. These three states compete with each other following a circular
403 hierarchy, as defoliated box trees 'lose' against box trees with foliage, which are in turn invaded by box tree moths,
404 which finally leads to defoliated box trees. Similar rock-paper-scissors games have been described in other ecological
405 contexts such as polymorphic bacterial strains [Kerr et al., 2002] and plant-mutualist-exploiter systems [Szilágyi
406 et al., 2009].

407 We also explore moth persistence over a larger range of fecundity and survival parameters than those estimated.
408 Predation on the moth and on the caterpillars is currently low [Kenis et al., 2013], in part because the box tree
409 moth accumulates boxwood alkaloids in its body [Leuthardt and Baur, 2013]. However, native predators may
410 become efficient to feed on the moth following phenotypic plasticity or adaptation [Carlsson et al., 2009]. Native
411 egg parasites like trichograms often used in biological control may also become able to feed on the moth, thereby
412 reducing its fecundity. We find that the moth could rapidly go extinct only for very low fecundity and survival rates
413 (lower-left corners of Figure 4a and f). It is therefore unlikely that the accommodation of native natural enemies
414 will trigger moth extinction.

415 One step further, hypothesis 1b postulates that long-term coexistence is due to asynchronous dynamics, and
416 that moth extinction is due to the synchronisation of the local dynamics. If we artificially ensure that the invasion
417 begins with a moth in each cell, we observe that all boxwood stands are defoliated simultaneously and that the
418 moth disappears globally in a dynamic of type pulse outbreak [Berryman, 1987]: perfect synchronization indeed
419 leads to moth extinction. But if all stands are initially invaded except a single one, this is enough for the occurrence
420 of desynchronisation, and the whole system becomes viable. The moth can therefore disappear due to perfect
421 synchronization, with 100% of the patches invaded simultaneously. However, any other mechanism that globally
422 reduces drastically the resources may also cause moth extinction. Indeed, with high moth fecundity and survival
423 rates (upper-right corners of Figure 4a and f) the moth depletes the resource until its own extinction. In contrast to
424 the results obtained with *H. spinipennis*-*A. dieffenbachii* system, our results indicate that global resource depletion
425 is responsible for moth extinction, rather than synchronisation of local dynamics [Johst and Schöps, 2003]. This
426 is in line with the individual-based model of Uchmański [2019], who found that forest insect pests may go extinct
427 when adult fecundity or larvae survival increase. Within the coexistence regime, the average density of moths and
428 the average intensity of the invasion are insensitive to moth fecundity and survival; the moth either persists at the
429 coexistence density or goes extinct (Figure 4).

430 Interestingly, the moth population can persist even when it periodically invades 99% of the patches (Figure 5
431 top), provided that leaves grow back fast enough to prevent global resource depletion. In this case the moth invades
432 a significant proportion of the patches even during troughs (about 12%); the cyclic dynamics are therefore getting
433 closer to a permanent outbreak [Berryman, 1987]. The same process occurred in the model of Uchmański [2019],
434 where leaf growth rate was expressed by a parameter defining the number of years needed for their regeneration.
435 In his model, when the leaf growth rate increased the dynamics of the cyclic outbreak was accelerated, with shorter
436 periods between peaks and troughs. The system then transitioned to a permanent outbreak for very rapid leaf growth

437 rates. On the contrary, a slow leaf growth rate led to the extinction of the insects (Figure 5).
438

439 Results for hypothesis 2

440 We further postulate that, despite local cycles of extinction and recolonization, the coexistence regime is stationary
441 at the landscape scale (hypothesis 2), a phenomenon called statistical stability [De Roos et al., 1991, Holyoak et al.,
442 2005, Amarasekare, 2008]. Instead, we find that the coexistence regime is periodic at the landscape scale (Figure
443 6a). A similar pattern has been observed in the *H. spinipennis*–*A. dieffenbachii* system [Johst and Schöps, 2003]
444 and in Uchmański [2019]. The global period ranges between 20 generations (high leaf growth rate, Figure 5 top) and
445 40 generations (low leaf growth rate, Figure 5 bottom). In contrast, the invasion of a local patch lasts 5 generations
446 when 1000 moths are introduced at once, and 7 generations when a single moth colonizes the patch (Figure 3).
447 This discrepancy between the local and global timescales suggests that periodicity at the global scale results from
448 the combination of the local time scale and the pace of dispersal. During peaks, between 60 and 99% of the box-
449 wood patches are simultaneously invaded by the moth, and 1-5% during periods of minimal abundance, depending
450 on parameter values. This corresponds to periodic travelling waves, which have been described in prey-predator
451 systems [Lambin et al., 1998, Sherratt, 2001]. However, such prey-predator systems are locally periodic as well,
452 and long-term coexistence does not require spatial structure. In contrast, in our study system, the periodic waves
453 emerge from the spatial structure, instead of being a mere consequence of local periodicity.
454 If the mean dispersal distance is very low (1 cell on average, keeping rare long-distance events), the amplitude of
455 the oscillations is also very low (Figure 7b) and the system tends to be statistically stable.

457 Results for hypothesis 3

458 Hypothesis 3 posits that asynchronous local dynamics require intermediate dispersal distance [Myers, 1976, Myers
459 and Campbell, 1976], because very limited dispersal might prevent suitable boxwood patches from colonization (3a),
460 whereas very long-distance dispersal may synchronize local dynamics (3b). However, with the measured parameter
461 values we find that the long-term probability of moth persistence is insensitive to dispersal distance. This is shown
462 in Figure 7a, where the measured value for the production of new leaves from wood after total defoliation r_0 equals
463 $5 * 10^{-3}$ (-2.3 on a log scale). In that case, the moths persist whatever the mean dispersal distance is (1, 25 or 70
464 cells), because boxwood produces new shoots after total defoliation fast enough to enable moth persistence even
465 when the global leaf biomass is low. Meanwhile, previously infected areas produce enough leaves to support another
466 moth outbreak. Conversely, when r_0 equals $2 * 10^{-3}$ (-2.7 on a log scale, which may happen under climatic stress
467 for instance), it turns out that the moth does not persist when the mean dispersal distance equals 70 cells (Figure
468 6b). The moth initially invades 99% of the patches (Figure 6c) and reaches very high densities (Figure 6d). This
469 reduces the global leaf biomass (Figure 6e) and the moth eventually collapses due to resource depletion. In the
470 case of coexistence (Figure 6a) the maximal % of invaded patches is around 60-70%, the maximal moth density is
471 3 times lower and the minimal leaf biomass is 5 times higher than in the extinction case.
472 We also find that when the mean dispersal distance is very short (1 cell on average) the probability of moth

473 persistence is not affected by the offshoot production rate. Because of short-distance dispersal, the moth does not
474 generate periods of global invasion and intact patches are always present at the border of its slow moving invasion
475 front. In that case, relatively high offshoot production rates are unnecessary as the moth do not rely on the new
476 growth of recently defoliated patches. In contrast, when the average dispersal distance is larger (e.g. 25 and 70
477 cells), the probability of persistence increases with the offshoot production rate (Figure 7a). In such cases, the moth
478 needs to recolonize recently defoliated patches because during peaks a large proportion of patches are defoliated at
479 the same time. Therefore, relatively high offshoot production rates are necessary to avoid global over-exploitation.

480 The influence of the mean dispersal distance on moth persistence is therefore studied with a relatively low
481 offshoot production rate, $r_0 = 2 * 10^{-3}$. As expected by hypothesis 3b, frequent long-distance dispersal events lead
482 to the extinction of the moth due to global resource depletion (Figure 7b, continuous line). This effect of long-
483 distance dispersal was not present in Uchmański [2019], this can be explained to the use of a thin-tailed Gaussian
484 kernel characterized by very rare long-distance dispersal events, thus insect pests could not reach the distant trees
485 which had time to regenerate after their last defoliation.

486 Furthermore, hypothesis 3a posits that the moth goes extinct in the case of limited dispersal, because it would
487 not be able to escape over-exploited patches. However, the fat-tailed dispersal kernel prevents such phenomenon:
488 even when the mean dispersal distance is very low (1 cell), the moth can persist thanks to frequent long-distance
489 dispersal events. Things change when we constrain dispersal to a uniform distribution, which ranges between 1 cell
490 and a given maximum of cells. In that case, when the maximum number of cells is low enough (up to 4 cells), the
491 moth invasion can get stuck in a landscape dead end and it disappears because of local resource depletion, and not
492 global resource depletion (Figure 7b, dotted line). Prey-predator systems subject to limit cycles was also stabilized
493 by limited dispersal in the individual-based model of Cuddington and Yodzis [2000], where limited dispersal reduced
494 the average predation rate and thereby avoided local instability. However, if dispersal is too limited the consumer
495 can go extinct because of a drastic reduction in the rate of predation, as is the case in our model when long distance
496 dispersal events are extremely rare due to uniform dispersal kernel (Figure 7b, dotted line).

497 The results obtained using the fat-tailed dispersal seems the most plausible, indeed rare long-distance dispersal
498 events mediated either by wind or by human dispersal likely occur in the case of the box tree moth. With a fat-tailed
499 dispersal kernel, multiple invasion fronts are created far away from invaded patches because long-distance dispersal
500 events are frequent [Shaw, 1995]. This created a fragmented landscape of defoliated and intact boxwood, in which
501 the moth does not end up in a dead end. Such a fragmented invasion front can be observed in Europe. The moth
502 was first observed in Germany in 2006/2007; in the same year it spread to Switzerland and the Netherlands. It
503 then spread to France [Feldtrauer et al., 2009] and the United Kingdom [Salisbury et al., 2012] in 2008, to Austria
504 in 2009, to Italy [Bella, 2013] in 2010, and to Portugal, Iran and Armenia in 2016 [Bras et al., 2019]. Long-distance
505 dispersal might be due to the boxwood trade between European countries, and probably to a much lesser extent by
506 the natural dispersal of moths. We therefore expect that in practise only frequent long-distance dispersal can lead
507 to the extinction of the moth, due to global resource depletion.

508 Results for hypothesis 4

509 Next, we predict that the coexistence regime depends on the landscape characteristics, in particular its size (4a)
510 and the proportion of suitable boxwood patches (4b). To do so, we use wrapped landscapes (with no edge effect) of

511 different sizes and different proportions of randomly distributed suitable patches (Figure 8a). Below 200*200 cells,
512 which corresponds to about 12 000 km², coexistence does not occur within the realistic range of parameter values,
513 because previously defoliated patches are quickly recolonized by the moth and lack time to grow back. This induces
514 a global resource collapse and drives the moth to extinction. Above the 200*200 threshold, the larger the landscape
515 is, the more likely the coexistence occurs, in line with hypothesis 4a. In the previous sections, we restrict our model
516 to the French Alps, but we expect that long term coexistence is even more likely on the European scale because
517 larger landscapes favor coexistence. The influence of landscape size is also apparent in the real landscape, with a
518 uniform and short-range dispersal kernel: when the invasion begins in a relatively isolated area of the landscape,
519 coexistence is impaired by small size.

520 A priori, the effect of the initial proportion of boxwood patches on coexistence is unclear (4b) because on the
521 one hand a higher proportion of suitable patches provides more resources to the moths, while on the other hand
522 it may trigger moth outbreaks which ultimately leads to resource depletion. We find that the latter mechanism
523 is on the driver's seat: reducing the proportion of boxwood patches increases the probability of moth persistence
524 (Figure 8a). More precisely, the landscapes larger than 400*400 cells filled with less than 20% of boxwood patches
525 almost always allow coexistence. In such cases, most dispersal events fail to find suitable patches, lowering the moth
526 population density, which in turn leaves more time for leaves to grow back. On the contrary, a high proportion of
527 suitable patches results in high moth densities which leads to global over-exploitation, despite a potentially higher
528 leaf biomass.

529 The coexistence regime has interesting consequences on the final proportion of boxwood patches, which corre-
530 sponds to the initial proportion minus the proportion of patches which wither completely due to over-exploitation.
531 Under coexistence, the final proportion increases linearly with the initial proportion with a weak slope of about 0.1,
532 whereas the slope is close to 1 in the case of moth extinction (Figure 8b). This indicates that the local extinction of
533 boxwood patches is not responsible for global moth extinction. Instead, the final proportion of boxwood patches is a
534 long-term consequence of coexistence and results from their gradual death (Figure 8c). During each moth outbreak,
535 a small proportion of the boxwood patches disappears due to over exploitation. Then, right after the outbreak a few
536 boxwood patches are recolonized from neighbouring patches (only previously occupied patches can be recolonized),
537 which induces a clustered distribution of the boxwood patches. As a result of clustering, the aggregation index is
538 always positive, which indicates that the landscapes created by long-term coexistence are more aggregated than
539 random landscapes. Boxwood patches relatively isolated in the initial landscape experience larger extinction rates
540 and create holes in the landscape. In contrast, areas where boxwood patches are initially more abundant persist
541 more often, which creates clusters. Moreover, the aggregation increases with the average moth dispersal distance
542 (Figure 8d). Boxwood patches favor moth outbreaks: increasing the boxwood patches proportion over the landscape
543 produces severe outbreaks. This induces apparent competition between boxwood patches because of their shared
544 pest. With low dispersal distance, apparent competition between patches is mainly local, which limits the forma-
545 tion of clusters. Instead, with high dispersal distance apparent competition is global and the aggregated pattern
546 results from the interplay between local facilitation (recolonization of boxwood patches is purely local) and global
547 competition, as in many spatially self-structured systems [Kéfi et al., 2007, 2008]. This is confirmed by simulations
548 where boxwood recolonization is global, in that case the aggregation process vanishes (details not shown).

549 We further explore how the aggregation process creates boxwood clusters of different sizes, for various dispersal

550 distance. To do so, we start with landscapes which are initially filled with boxwood patches, and run simulations
551 after invasion by the moth. At the end of the simulations, we fit a power-law model to the final distribution of the
552 cluster sizes (Figure 9 top). Clusters smaller than 5 boxwood patches are excluded from the fit. We find that small
553 dispersal distance leads to a cluster size distribution closer to a power-law than large dispersal distance. When the
554 dispersal distance is large (10 to 50 cells), the cluster size distribution follows a truncated power law (Figure 9 top),
555 which indicates that large clusters are under-represented. Large dispersal distance leads to an increase of herbivory,
556 which produces two distinct effects. On the one hand, it favors aggregation due to global apparent competition, as
557 discussed earlier (Figure 8d). On the other hand, it increases the death rate of boxwood patches and thus reduces
558 the final proportion of patches in the landscape (Figure 8e). This is why under large dispersal distance (10 to 50
559 cells) the final landscapes has a homogeneous aspect of equally spaced small clusters (Figure 9 bottom).

560 These regular patterns are similar to Turing instabilities [Turing, 1990, Murray, 2001] and result from "scale-
561 dependent feedbacks" which combine short-distance positive feedbacks and long-distance negative feedbacks [Rietk-
562 erk and van de Koppel, 2008]. In the present case, short-distance positive feedback correspond to local facilitation
563 of boxwood due to recruitment while apparent competition between boxwood stands because of their shared pest
564 mirror long-distance negative feedbacks. Several studies have investigated how spatial patterns can emerge from
565 such scale-dependent feedbacks in a variety of ecological scenarios, such as plant-water interactions [Klausmeier,
566 1999, von Hardenberg et al., 2001, Rietkerk et al., 2002, Meron et al., 2004, Kéfi et al., 2010], plant-plant interactions
567 [Lejeune et al., 1999], or predator-prey interactions [Levin and Segel, 1976, Solé and Bascompte, 2012]. It has been
568 shown that such spatial patterns emerge in predator-prey systems when the predator has a larger dispersal capacity
569 than the prey [Gurney et al., 1998, de Roos et al., 1998]. We demonstrate here that this can also be the case in the
570 context of a plant-herbivore system, using a model calibrated empirically.

571 Implications for management

572

573 First, the most important finding for management purposes is that the moth heavily impacts boxwood stands. With
574 the estimated parameter values, we find that in the study area only 15% of the initial boxwood biomass remains
575 (Figure 4b) and that 48% of the original boxwood patches completely disappear (Figure 4c), which represents 2414
576 square kilometres in the French Alps. Under low moth fecundity and high caterpillar survival, the moths could
577 persist longer in heavily defoliated patches. The severe decrease in box tree biomass can impact the many species
578 associated with boxwood, as well as the ecosystem services provided by the shrub (i.e sediment trapping and water
579 storage) [Mitchell et al., 2018]. In stands where boxwood is severely weakened or extinguished, recolonization by
580 neighbouring patches may be prevented by pioneer plants, potentially other invasive species such as *Buddleja davidii*
581 or *Ailanthus altissima*, in a kind of 'invasion meltdown' process [Simberloff and Holle, 1999].

582 Next, the periodic invasion dynamics can lead to confusion regarding the persistence of the box tree moth.
583 A period of low overall abundance should not be confused with a decrease in invasion, and moth control methods
584 should take periodic invasion dynamics into account. Remote sensing methods may be appropriate in order to detect
585 the few boxwood stands that provide refuge under low moth abundance [Kerr and Ostrovsky, 2003]. We suggest
586 that detecting stands of undefoliated boxwood that allow moth persistence during a period of low abundance could

587 provide an interesting management strategy, since control efforts could be increased on these particular patches.

588 Finally, management actions might consider preventing anthropogenic long-distance dispersal. However, we find
589 that only very limited dispersal could lead to moth extinction, which occurs with a uniform distribution of dispersal
590 events of no more than 4 cells (Figure 7b, dotted line). As soon as dispersal is higher, the moth could escape
591 dead ends in the landscape and therefore persists. Even if anthropogenic long-distance dispersal is prevented, a
592 few natural long-distance dispersal events might ensure moth persistence. It is therefore unlikely that management
593 actions limiting dispersal can be able to eradicate the moth. However, such actions can reduce the impact on
594 boxwood stands, since we find that long-distance dispersal increases the extinction rate of boxwood patches (Figure
595 8e).

596 Three scenarios may occur after the invasion of box tree moth in Europe: extinction of both species, extinction
597 of the moth only, or coexistence. Our theoretical approach combined with field and experimental data suggests
598 that coexistence is the most likely outcome, with cycles of moth outbreaks and crashes. Coexistence comes along
599 with a severe reduction of boxwood biomass at the landscape scale: boxwood stands may therefore become closer
600 to brown than green. Moth extinction can also occur, which indicates that the invasion dynamics of exotic pests
601 can be mitigated even in the absence of predators and effective plant defenses.

602 We further show that plant-herbivore coexistence through spatial effects does not require poorly mobile wing-
603 less species, as in our model a wide range of dispersal values result in coexistence. Coexistence occurs in large
604 landscapes, long-distance dispersal thus requires a spatial scaling-up for the persistence of the system. Particularly
605 intense long-distance dispersal nevertheless leads to herbivore extinction, provided that plant grows back slowly.
606 In that case, the herbivore depletes its resources at the global scale, which leads to its own extinction even with-
607 out a complete synchronization of the local dynamics. Finally, coexistence is easier in patchy landscapes because
608 unsuitable patches increase moth mortality during dispersal and thereby reduce the global insect population size.
609 Interestingly, when plants disperse locally the spatial dynamics of the system lead to the formation of such a patchy
610 landscape, with relatively small plant patches evenly distributed in the landscape. The system thus creates its own
611 stability conditions.

612 Acknowledgements

613 • We thank all the student interns who participated in both field and experimental work: Aristide Chauveau,
614 Alison Dilien, Jessica Barbe and Océane Guillot. We also thank Elisabeth Tabone and Thomas Defferier
615 (INRAE) for their mass measurements on their farmed caterpillars, and Audrey Bras (INRAE) for the flight
616 distance data and fruitful exchanges.

617 • This article is financially supported by AAP USMB and FREE federation. The PhD scholarship of L. Ledru
618 is funded by the French Ministry for Education and Research. J. Garnier acknowledges NONLOCAL project
619 (ANR-14-CE25-0013), GLOBNETS project (ANR-16-CE02-0009) and the European Research Council (ERC)
620 under the European Unions Horizon 2020 research and innovation programme (grant agreement no. 639638,
621 MesoProbio).

622 References

- 623 Ahmed, D., Choudhary, M.I., Turkoz, S., and Sener, B. (1988) Chemical constituents of *Buxus sempervirens*.
624 - *Planta Med.* 54:173–174.
- 625 Amarasekare, P. (2008) Spatial Dynamics of Foodwebs. - *Annu. Rev. Ecol. Evol. S.* 39: 479–500.
- 627 Bella, S. (2013) The box tree moth *Cydalima perspectalis* (walker, 1859) continues to spread in southern
628 Europe: new records for Italy (*lepidoptera pyraloidea crambidae*). - *Redia* 96: 51–55.
- 630 Berryman, A.A. (1987) The theory and classification of outbreaks. - In: *Insect Outbreaks*. Academic press
631 Inc., pp.3-30.
- 633 Blackburn, T.M., Pyšek, P., Bacher, S., Carlton, J.T., Duncan, R.P., Jarošík, V., Wilson, J.R. and Richard-
634 son, D.M. (2011) A proposed unified framework for biological invasions. - *Trends Ecol. Evol.* 26: 333–339.
- 636 Bras, A., Avtzis, D.N., Kenis, M., Li, H., Véték, G., Bernard, A., Courtin, C., Rousselet, J., Roques, A. and
637 Auger-Rozenberg, M.A. (2019) A complex invasion story underlies the fast spread of the invasive box tree
638 moth (*cydalima perspectalis*) across Europe. - *J. Pest. Sci.* 92(3): 1187-1202.
- 640 Carlsson, N.O., Sarnelle, O. and Strayer, D.L. (2009) Native predators and exotic prey –an acquired taste ?.
641 - *Front. Ecol. Environ.* 7: 525–532.
- 643 Comins, H.A. and Hassell, M.P. (1996) Persistence of multispecies host–parasitoid interactions in spatially
644 distributed models with local dispersal. - *J. Theor. Biol.* 183: 19–28.
- 646 Cuddington, K.M. and Yodzis, P. (2000) Diffusion-Limited Predator-Prey Dynamics in Euclidean Environ-
647 ments. - *Theor. Popul. Biol.* 58: 259-278.
- 649 De Roos, A.M., McCauley, E. and Wilson, W.G. (1991) Mobility versus density-limited predator-prey dy-
650 namics on different spatial scales. - *Proc. Royal Soc. B* 246: 117-122.
- 652 De Roos, A.M., McCauley, E. and Wilson, W.G. (1998) Pattern Formation and the Spatial Scale of Interac-
653 tion between Predators and Their Prey. - *Theor. Popul. Biol.* 53:108-130.
- 655 Denno, R.F., Lewis, D. and Gratton, C. (2005) Spatial variation in the relative strength of top-down and
656 bottom-up forces: causes and consequences for phytophagous insect populations. - *Ann. Zool. Fenn.* 295–311.
- 658 Devkota, K.P., Lenta, B.N., Fokou, P.A. and Sewald, N. (2008) Terpenoid alkaloids of the *Buxaceae* family
659 with potential biological importance. - *Nat. Prod. Rep.* 25: 612–630.
- 661 Domenico, F., Lucchese, F. and Magri, D. (2012) *Buxus* in Europe: Late quaternary dynamics and modern
662 vulnerability. - *Perspect. Plant. Ecol.* 14: 354–362.
- 664 Eber, S. and Brandl, R. (1996) Metapopulation dynamics of the tephritid fly *Urophora cardui*: an evaluation
665 of incidence-function model assumptions with field data. - *J. Anim Ecol.* 621–630.
- 667

668 Feldtrauer, J.-F., Feldtrauer, J.J. and Brua, C. (2009) Premiers signalements en France de la pyrale du buis *di-*
669 *aphania perspectalis* (Walker, 1859), espèce exotique envahissante s'attaquant aux buis (*Lepidoptera, Crambidae*).
670 - Bull. Soc. Entomol. Mulhouse. 65: 55–58.

671 Fox, J.W., Vasseur, D., Cotroneo, M., Guan, L. and Simon, F. (2017) Population extinctions can increase
672 metapopulation persistence. - Nat. Ecol. Evol. 1:1271–1278.

674 Gillespie, R.G., Baldwin, B.G., Waters, J.M., Fraser, C.I., Nikula, R. and Roderick, G.K. (2012) Long-distance
675 dispersal: a framework for hypothesis testing. - Trends Ecol. Evol. 27: 47–56.

677 Göttig, S. and Herz, A. (2016) Are egg parasitoids of the genus *Trichogramma* (*Hymenoptera: Trichogram-*
678 *matidae*) promising biological control agents for regulating the invasive Box tree pyralid, *Cydalima perspec-*
679 *talis* (*Lepidoptera: Crambidae*)?. - Biocontrol Sci. and Techn. 26: 1471–1488.

681 Göttig, S. (2017) Development of eco-friendly methods for monitoring and regulating the box tree pyralid,
682 *Cydalima perspectalis* (*Lepidoptera: Crambidae*), an invasive pest in ornamentals, PhD thesis, Technische
683 Universität.
684

685 Göttig, S. and Herz, A. (2017) Observations on the seasonal flight activity of the box tree pyralid *Cydalima*
686 *perspectalis* (*Lepidoptera: Crambidae*) in the Rhine-Main Region of Hesse. Journal of Cultivated Plants. 69:
687 157–165.
688

689 Göttig, S. and Herz, A. (2018) Susceptibility of the Box tree pyralid *Cydalima perspectalis* Walker (*Lepi-*
690 *doptera: Crambidae*) to potential biological control agents Neem (NeemAzalR©-T/S) and entomopathogenic
691 nematodes (NemastarR©) assessed in laboratory bioassays and field trials. - J. Plant. Dis. Protect. 125:
692 365–375.
693

694 Gurney, W.S.C., Veitch, A.R., Cruickshank, I. and McGeachin, G. (1998) Circles and Spirals: Population
695 Persistence in a Spatially Explicit Predator-Prey Model. - Ecology. 79: 2516.
696

697 Hairston, N.G., Smith, F.E. and Slobodkin, L.B. (1960) Community structure, population control, and com-
698 petition. - Am. Nat. 94: 421–425.
699

700 Halley, J.M. and Dempster, J.P. (1996) The Spatial Population Dynamics of Insects Exploiting a Patchy Food
701 Resource: A Model Study of Local Persistence. - J Appl Ecol. 33: 439–454.
702

703 Hanski, I. and Gilpin, M.E. (1997) Metapopulation biology. - CA: Academic press, San Diego.
704

705 Harary, F. and Harborth, H. (1976) Extremal animals. - J. Combinator. Inform. Syst. Sci. 1: 1–8.
706

707 Harrison, S., Thomas, C.D. and Lewinsohn, T.M. (1995) Testing a metapopulation model of coexistence in
708 the insect community on ragwort (*Senecio jacobaea*). - Am. Nat. 145: 546–562.
709

710 Hassell, M.P., Comins, H.N. and May, R.M. (1991) Spatial structure and chaos in insect population dynam-
711 ics. - Nature. 353: 255–258.
712
713

714 Holyoak, M. and Lawler, S.P. (1996) Persistence of an extinction-prone predator-prey interaction through
715 metapopulation dynamics. - *Ecology*. 77: 1867–1879.

716 Holyoak, M., Leibold, M.A. and Holt, R.D. (2005) *Metacommunities: Spatial Dynamics and Ecological Com-*
717 *munities*. – University of Chicago Press.

719 Johst, K., Brandl, R. and Eber, S. (2002) Metapopulation persistence in dynamic landscapes: The role of
720 dispersal distance. - *Oikos*. 98: 263–270.

722 Johst, K. and Schöps, K. (2003) Persistence and conservation of a consumer–resource metapopulation with
723 local overexploitation of resources. - *Biol. Conserv.* 109: 57–65.

725 Kang, Y. and Armbruster, D. (2011) Dispersal effects on a discrete two-patch model for plant–insect interac-
726 tions. - *J. Theor. Biol.* 268: 84–97.

728 Kawazu, K., Nakamura, S. and Adati, T. (2010) Rearing of the box tree pyralid, *Glyphodes perspectalis*, larvae
729 using an artificial diet. - *Appl. Entomol. Zool.* 45: 163–168.

731 Kéfi, S., Rietkerk, M., van Baalen, M. and Loreau, M. (2007) Local facilitation, bistability and transitions in
732 arid ecosystems. - *Theor. Popul. Biol.* 71: 367–379.

734 Kéfi, S., van Baalen, M., Rietkerk, M. and Loreau, M. (2008). Evolution of Local Facilitation in Arid Ecosys-
735 tems. - *Am. Nat.* 172: E1–E17.

737 Kéfi, S., Eppinga, M.B., de Ruiter, P.C. and Rietkerk, M. (2010) Bistability and regular spatial patterns in
738 arid ecosystems. - *Theor. Ecol.* 3: 257–269.

740 Kenis, M., Nacambo, S., Leuthardt, F.L.G., Domenico, F.D. and Haye, T. (2013) The box tree moth, *Cy-*
741 *dalima perspectalis*, in Europe: horticultural pest or environmental disaster ?. - *Aliens: The Invasive Species*
742 *Bulletin.* 33: 38–41.

744 Kerr, B., Riley, M.A., Feldman, M.W. and Bohannan, B.J. (2002) Local dispersal promotes biodiversity in a
745 real-life game of rock–paper–scissors. - *Nature*. 418: 171–174.

747 Kerr, J. and Ostrovsky, M. (2003) From space to species: Ecological applications for remote sensing. - *Trends*
748 *Ecol. Evol.* 18: 299–305.

750 Klausmeier, C.A. (1999) Regular and Irregular Patterns in Semiarid Vegetation. - *Science*. 284: 1826–1828.

752 Klein, E.K., Lavigne, C. and Gouyon, P.H. (2006) Mixing of propagules from discrete sources at long distance:
753 Comparing a dispersal tail to an exponential. - *BMC Ecol.* 6: 3.

755 Lambin, X., Elston, D.A., Petty, S.J. and MacKinnon, J.L. (1998) Spatial asynchrony and periodic travelling
756 waves in cyclic populations of field voles. - *P. Roy. Soc. B-Biol. Sci.* 265: 1491–1496.

758 Lejeune, O., Couteron, P. and Lefever, R. (1999) Short range co-operativity competing with long range inhi-
759 bition explains vegetation patterns. - *Acta Oecol.* 20: 171–183.

760

761 Leuthardt, F. and Baur, B. (2013) Oviposition preference and larval development of the invasive moth *Cy-*
762 *dalima perspectalis* on five european box-tree varieties. - J. Appl. Entomol. 137: 437–444.

764 Leuthardt, F.L., Glauser, G. and Baur, B. (2013) Composition of alkaloids in different box tree varieties and
765 their uptake by the box tree moth *Cydalima perspectalis*. - Chemoecology 23: 203–212.

767 Levin, S.A. and Segel, L.A. (1976) Hypothesis for origin of planktonic patchiness. - Nature. 259:659-659.

769 Loru, F., Duval, D., Aumelas, A., Akeb, F., Guédon, D. and Guedj, R. (2000) Four steroidal alkaloids from
770 the leaves of *Buxus sempervirens*. - Phytochemistry. 54: 951–957.

772 Mally, R. and Nuss, M. (2010) Phylogeny and nomenclature of the box tree moth, *Cydalima perspectalis*
773 (Walker, 1859) comb. n., which was recently introduced into Europe (*Lepidoptera: Pyraloidea: Crambidae:*
774 *Spilomelinae*). - Eur. J. Entomol. 107: 393–400.

776 Maruyama, T. and Shinkaji, N. (1987) Studies on the life cycle of the box-tree pyralid, *Glyphodes perspectalis*
777 (walker)(*lepidoptera: Pyralidae*). I. seasonal adult emergence and developmental velocity. - Jpn. J. Appl.
778 Entomol. Z. 31: 226–232.

780 Maruyama, T. and Shinkaji, N. (1991) The life-cycle of the box-tree pyralid, *glyphodes perspectalis* (walker)(*lepidoptera:*
781 *Pyralidae*). II. developmental characteristics of larvae. - Jpn. J. Appl. Entomol. Z. 35: 221–230.

783 Melbourne, B., Cornell, H.V., Davies, K.F., Dugaw, C.J., Elmendorf, S., Freestone, A.L., Hall, R.J., Har-
784 rison, S., Hastings, A., Holland, M. and Holyoak, M. (2007) Invasion in a heterogeneous world: resistance,
785 coexistence or hostile takeover ?. - Ecol. Lett. 10: 77–94.

787 Meron, E. Gilad, E., von Hardenberg, J., Shachak, M. and Zarmi, Y. (2004) Vegetation patterns along a
788 rainfall gradient. - chaos soliton fract. 19: 367-376.

790 Mitchell, R., Chitanava, S., Dbar, R., Kramarets, V., Lehtijärvi, A., Matchutadze, I., Mamadashvili, G., Mat-
791 siakh, I., Nacambo, S., Papazova-Anakieva, I. and Sathyapala, S. (2018) Identifying the ecological and societal
792 consequences of a decline in *Buxus* forests in Europe and the Caucasus. - Biol. Invasions. 20: 3605–3620.

794 Murray, J.D. (2001) Spatial Pattern Formation with Reaction Diffusion Systems. - In: Mathematical biology
795 II. Springer-Verlag, pp.71-130.

797 Myers, J.H. (1976) Distribution and Dispersal in Populations Capable of Resource Depletion. A Simulation
798 Model. - Oecologia. 23: 255-269.

800 Myers, J.H. and Campbell, B.J. (1976) Distribution and dispersal in populations capable of resource deple-
801 tion. - Oecologia. 24: 7-20.

803 Nacambo, S., Leuthardt, F.L., Wan, H., Li, H., Haye, T., Baur, B., Weiss, R.M. and Kenis, M. (2014) Devel-
804 opment characteristics of the box-tree moth *Cydalima perspectalis* and its potential distribution in Europe. -
805 J. Appl. Entomol. 138: 14–26.

806

807 Nachman, G. (1988) Regional persistence of locally unstable predator/prey populations. - Exp. Appl. Acarol.
808 5: 293–318.

809

810 Palmqvist, E. and Lundberg, P. (1998) Population extinctions in correlated environments. - Oikos. 359–367.
811

812 Polis, G.A. (1999) Why are parts of the world green ? Multiple factors control productivity and the distribu-
813 tion of biomass. - Oikos. 3–15.

814

815 Rietkerk, M. and van de Koppel, J. (2008) Regular pattern formation in real ecosystems. - Trends Ecol. Evol.
816 23: 169-175.

817

818 Rietkerk, M., Boerlijst, M.C., van Langevelde, F., HilleRisLambers, R., van de Koppel, J., Kumar, L., Prins,
819 H.H.T. and de Roos, A.M. (2002) Self-organization of vegetation in arid ecosystems. - Am. Nat. 160: 524-530.

820

821 Salisbury, A., Korycinska, A. and Halstead, A.J. (2012) The first occurrence of larvae of the box tree moth,
822 *Cydalima perspectalis* (Lepidoptera: Crambidae) in private gardens in the uk. - Brit. J. Ent. Nat. Hist. 25:
823 1.

824

825 Santi, F., Radeghieri, P., Sigurta, G.I. and Maini, S. (2015) Sex pheromone traps for detection of the invasive
826 box tree moth in Italy. - B. Insectol. 68: 158-160.

827

828 Schöps, K. (2002) Local and regional dynamics of a specialist herbivore: overexploitation of a patchily dis-
829 tributed host plant. - Oecologia. 132: 256–263.

830

831 Shaw, M.W. (1995) Simulation of population expansion and spatial pattern when individual dispersal distri-
832 butions do not decline exponentially with distance. - Proc. Royal Soc. B. 259: 243-248.

833

834 Sherratt, J.A. (2001) Periodic travelling waves in cyclic predator–prey systems. - Ecol. Lett. 4: 30–37.
835

836 Simberloff, D. and Holle, B. (1999) Positive interactions of nonindigenous species: Invasional meltdown ? -
837 Biol. Invasions 1: 12.

838

839 Slansky Jr, F. and Scriber, J. (1982) Selected bibliography and summary of quantitative food utilization by
840 immature insects. - Bull. Ecol. Soc. Am. 28: 43–56.

841

842 Solé, R. and Bascompte, J. (2012) Spatial Self-Organization From Pattern to Process. - In: Self-Organization
843 in Complex Ecosystems. Princeton University Press, pp.65-125.

844

845 Stelter, C., Reich, M., Grimm, V. and Wissel, C. (1997) Modelling Persistence in Dynamic Landscapes:
846 Lessons from a Metapopulation of the Grasshopper *Bryodemus tuberculata*. - J. Anim. Ecol. 66: 508–518.

847

848 Szilágyi, A., Scheuring, I., Edwards, D.P., Orivel, J. and Yu, D.W. (2009) The evolution of intermediate
849 castration virulence and ant coexistence in a spatially structured environment. - Ecol. Lett. 12: 1306–1316.

850

851 Taylor, A.D. (1991) Studying metapopulation effects in predator-prey systems. - Biol. J. Linnean. Soc. 42:
852 305–323.

853

854 Tschamtkke, T. and Brandl, R. (2004) Plant-insect interactions in fragmented landscapes. - Annu. Rev. En-
855 tomol. 49: 405–430.

857 Van der Meijden, E. (1979) Herbivore exploitation of a fugitive plant species: local survival and extinction of
858 the cinnabar moth and ragwort in a heterogeneous environment. - Oecologia. 307–323.

860 Turing, A.M. (1990) The chemical basis of morphogenesis. - Bull. Math. Biol. 52: 153-197.

862 Uchmański, J. (2019) Cyclic outbreaks of forest insects: A two-dimensional individual-based model. - Theor.
863 Popul. Biol. 128: 1-18.

865 Van der Meijden, E. and Van der Veen-van, C. A. (1997) Tritrophic metapopulation dynamics: a case study
866 of ragwort, the cinnabar moth, and the parasitoid *Cotesia popularis*. - In: Metapopulation Biology. CA:
867 Academic press, pp.387–405.

869 Van der Straten, M. and Muus, T. (2010) The box tree pyralid, *Glyphodes perspectalis* (lepidoptera: Cram-
870 bidae), an invasive alien moth ruining box trees. Proc. Neth. Soc. Meet. 21: 107–111.

872 von Hardenberg, J., Meron, E., Shachak, M. and Zarmi, Y. (2001) Diversity of Vegetation Patterns and
873 Desertification. - Phys. Rev. 87: 198101.

875 Wan, H., Haye, T., Kenis, M., Nacambo, S., Xu, H., Zhang, F. and Li, H. (2014) Biology and natural enemies
876 of *Cydalima perspectalis* in Asia: Is there biological control potential in Europe ?. - J. Appl. Entomol. 138:
877 715–722.

879 Wilkinson, D.M. and Sherratt, T.N. (2016) Why is the world green ? The interactions of top-down and
880 bottom-up processes in terrestrial vegetation ecology. - Plant Ecol. Divers. 9: 127–140.

882 Wilson, R.J. and Thomas, C.D. (2002) Dispersal and the spatial dynamics of butterfly populations. - In:
883 Dispersal ecology. Blackwell Science, pp.257–278.

885 Winder, L., Alexander, C.J., Holland, J.M., Woolley, C. and Perry, J.N. (2001) Modelling the dynamic
886 spatio-temporal response of predators to transient prey patches in the field. - Ecol. Lett. 4: 568–576.

887

Tables

Table 1: Model parameters. The values correspond to those most representative of actual ecological conditions. The parameters are either measured quantitatively, i.e. a direct value of the parameter concerned is measured, or qualitatively, i.e. the measurement of a process allows the calibration of the associated parameter. We estimate the unmeasured parameters from the model simulations, and aim to be consistent with the ecological situation. The parameters obtain from the literature come from : f [Kawazu et al., 2010, Wan et al., 2014], α [Slansky Jr and Scriber, 1982], $S_{m,max}$ [Kawazu et al., 2010]. The source listed as "experiment" corresponds to the measurements of moth weights made by the INRAE for α , and the mesocosm experiment for σ_m , σ_l and $S_{m,max}$. "Flight carousel experiment" corresponds to the measurements made by Bras et al. from the INRAE.

	Settings	Measured	Values	Unit	Meaning	Source
Leaves	v	No	0.98	$\frac{1}{t}$	Leaf survival rate at senescence	estimate
	r_f	No	0.4	$\frac{1}{t}$	Leaf growth rate	estimate
	L_{max}	No	$\frac{1}{3}W_{max}$	$g.ha^{-1}$	Leaf carrying capacity	estimate
	r_0	Quantitative	$5 * 10^{-3}$	$\frac{1}{t}$	Offshoot production rate	field
	σ_l	Qualitative	0.01	-	Consumption function setting	experiment
Wood	W_{max}	No	$3 * 10^9$	$g.ha^{-1}$	Wood carrying capacity	estimate
	d_{max}	Quantitative	0.74	-	Saturation value of the maximum mortality function $D_{max}(\rho)$	field
	β_s	No	10	-	Setting of the wood mortality function by consumption (curvature)	estimate
	θ_s	No	1.2	-	Setting of the wood mortality function by consumption (inflection point)	estimate
	β_r	No	5	-	Setting of the wood growth function (curvature)	estimate
	θ_r	No	$5 * 10^{-5}$	-	Setting of the wood growth function (inflection point)	estimate
	$r_{w,max}$	Qualitative	0.3	-	Saturation value of the wood growth function	field
	$r_{w,min}$	No	1	-	Saturation value of the growth deficit function γ_0	estimate
	d	No	0.95	-	Setting of the growth deficit function γ_0	estimate
	ω_1	No	0.1	-	Setting of the wood dispersal function	estimate
	ω_{max}	No	$1 * 10^{-5}$	-	Maximum proportion of wood that can contribute to dispersal	estimate
Box tree moth	f	Quantitative	120	individual	Box tree moth fecundity	literature
	α	Quantitative	0.3	g	Amount of leaf needed by a box tree moth for its larval cycle	literature and experiment
	σ_m	Qualitative	0.85	-	Setting of caterpillar survival function	experiment
	$S_{m,max}$	Quantitative	0.49	$\frac{1}{t}$	Maximum caterpillar survival rate	literature and experiment
	s	No	0.4	$\frac{1}{t}$	Survival rate of adults (moths)	estimate
	$M_{m,max}$	No	0.01	$\frac{1}{t}$	Survival rate of adults during dispersal	estimate
	δ	No	0.01	-	Parameter of the dispersal function	estimate
	c	Qualitative	0.5	-	Tail shape parameter of the Exponential power distribution	flight carousel experiment
α_d	Quantitative	25	cells	Average dispersal distance of the Exponential power distribution	flight carousel experiment	

888 Figure legends

889 **Fig. 1** Model of dynamics between the boxwood, separated into wood and leaves, and the box tree moth. The
890 arrows show the interaction between the three variables

891 **Fig. 2** Main results of mesocosm manipulation with measurement of defoliation intensity and box tree moth sur-
892 vival according to competition for the resource μ . (a) leaf consumption function $\frac{S_l(\mu)}{v}$. (b) box tree moth survival
893 function $S_m(\mu)$.

894 **Fig. 3** Visualization of invasion dynamics in the local model. Simulation with ecologically realistic parameters
895 given in Table 1

896 **Fig. 4** Final state maps in the real landscape in function of fertility f and maximum survival $S_{m,max}$. (a)
897 landscape-scale probability of moth persistence, (b) landscape-scale wood biomass expressed as a percentage of
898 the landscape-scale carrying capacity, (c) number of boxwood patches disappearing as a percentage of the initial
899 number of boxwood patches, (d) landscape-scale moth biomass, (e) number of patches invaded as a percentage of
900 the number of boxwood patches present, (f) time of moth persistence. The ecologically realistic parameter values
901 are $f = 120$ and $S_{m,max} = 0.5$.

902 **Fig. 5** Effect of the leaf intrinsic growth rate on the mean percentage of invaded patches. The percentage drop
903 to zero when the moth do not persist in these conditions (when $r_f < 0.22$). The two inserts show the invasion
904 dynamics for two growth rate values.

905 **Fig. 6** Example of global population dynamics in the case of coexistence (a) and moth collapse (b). (c) maximum
906 % of invaded patches. (d) maximum moth biomass. (e) minimum leaf biomass. Parameters values as in Table 1,
907 except for $r_0 = 2 * 10^{-3}$ and for the average dispersal distance α_d which either equals 5 cells (moth persistence) or
908 70 cells (moth collapse)

909 **Fig. 7** (a) Effect of the rate of new leaves production by the wood (r_0) on the probability of moth persistence. For
910 each tested value, the probability of persistence is obtained by 50 simulations conduct on the realistic landscape with
911 random initial patch of invasion. Three average dispersal distances are tested, a realistic distance of 25 cells, a very
912 short distance of one cell, and a very large distance of 70 cells. (b) Effect of the average dispersal distance on the
913 probability of moth persistence. For each tested value, the probability of persistence is obtained by 50 simulations
914 conduct on the realistic landscape with random initial patch of invasion. Each time two dispersal functions are
915 tested: a fat-tailed function, and an uniform function. The minimum dispersal distance is one cell. The inserts
916 show the percentage of patch invaded over time for three selected average dispersal distances of 1, 5 and 70 cells
917 with the fat tail dispersal function.

918 **Fig. 8** Simulation in theoretical landscapes. (a) The probability of moth persistence depends on space size and on
919 the initial proportion of boxwood patches. (b) In the case of coexistence, the final proportion of boxwood patches
920 is much lower than the initial proportion because moth outbreaks cause patch extinctions. (c) The boxwood pro-
921 portion in the landscape declines during each moth outbreak. (d) The aggregation index increases along with the
922 average dispersal distance. (e) In coexistence, increasing the dispersal distance reduces the final proportion of box-
923 wood patches in the landscape. All other parameter values are set to the realistic values.

924 **Fig. 9** Effect of moth dispersal distance (increasing from left to right) on the size distribution of boxwood clusters
925 at the end of the simulations (5000 time steps), in large theoretical landscapes of 550*550 cells. Top: regression

926 lines correspond to the fit to a power-law distribution. The first size class (black square) has been excluded from
927 the regression. Bottom : snapshot of the landscape at the end of the simulation, black cells indicate live boxwood
928 patches. All other parameter values are set to the realistic values.

929

Figures

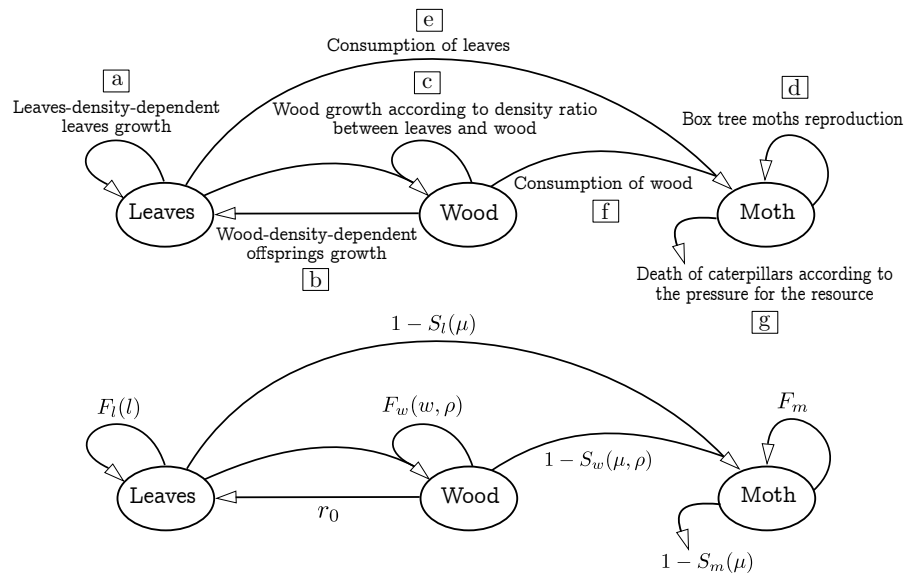


Figure 1

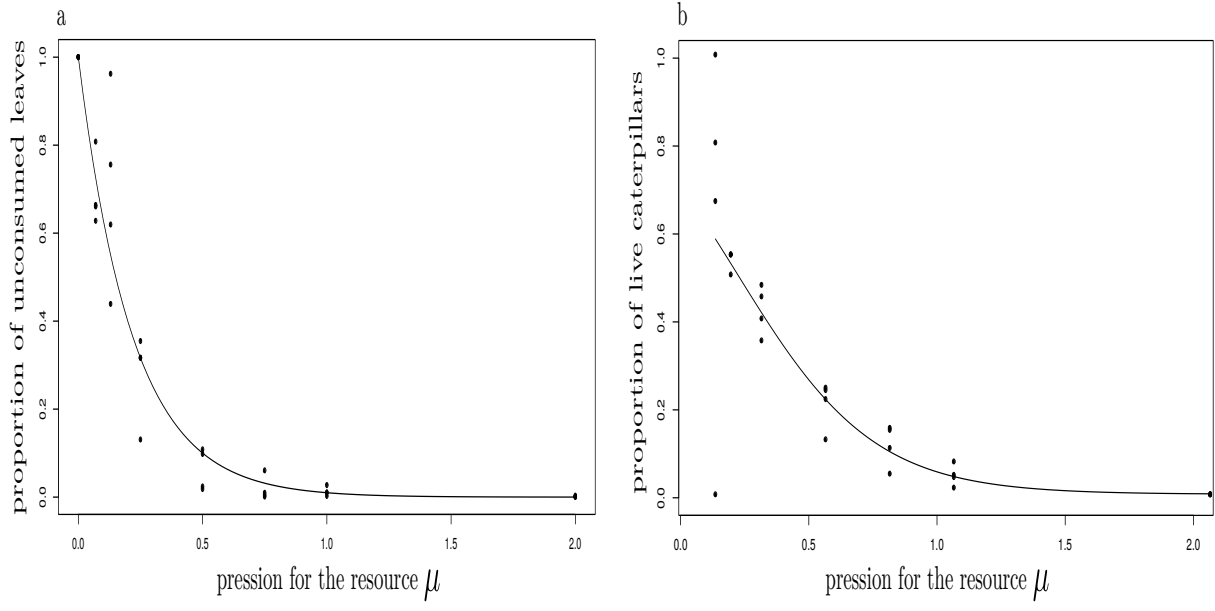


Figure 2

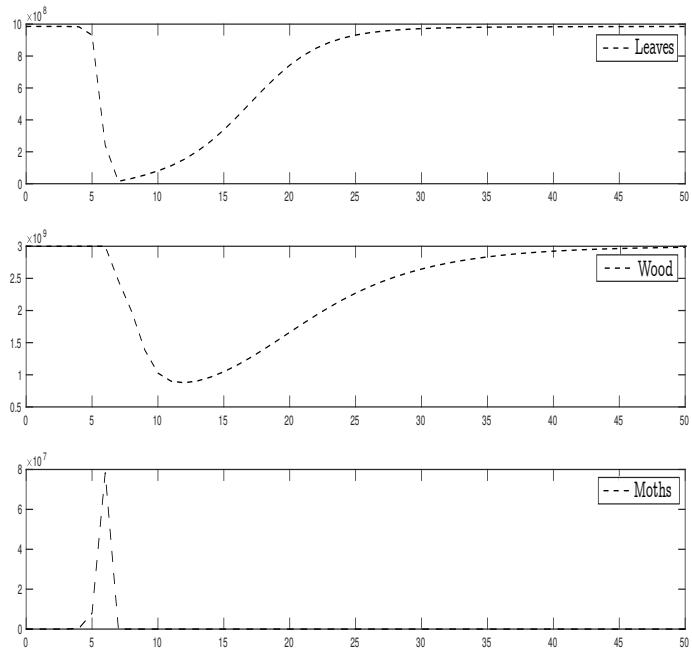


Figure 3

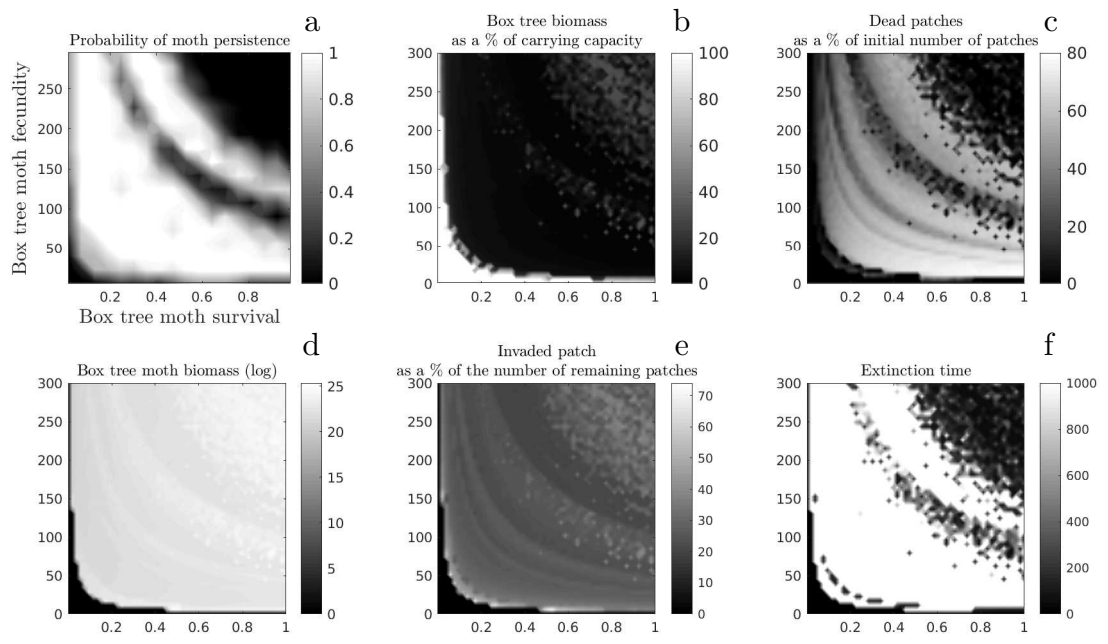


Figure 4

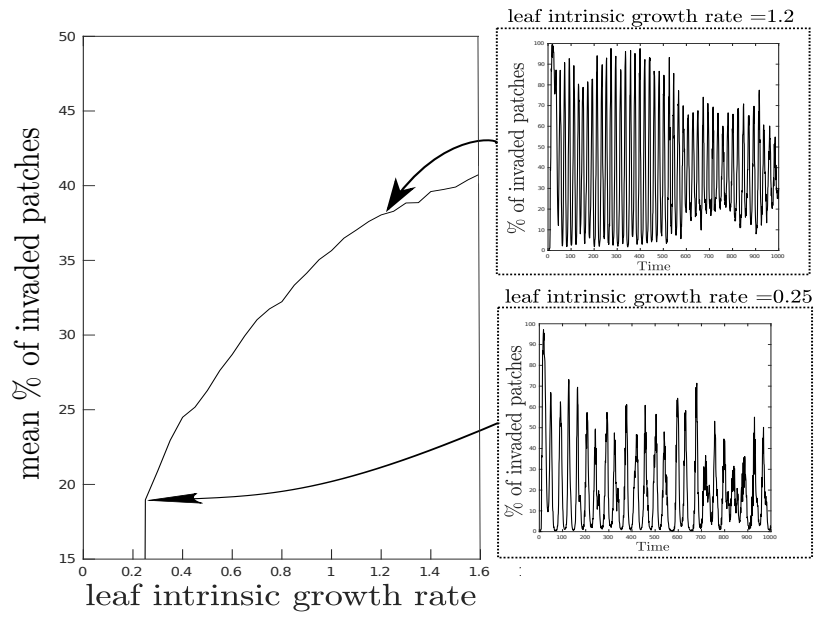


Figure 5

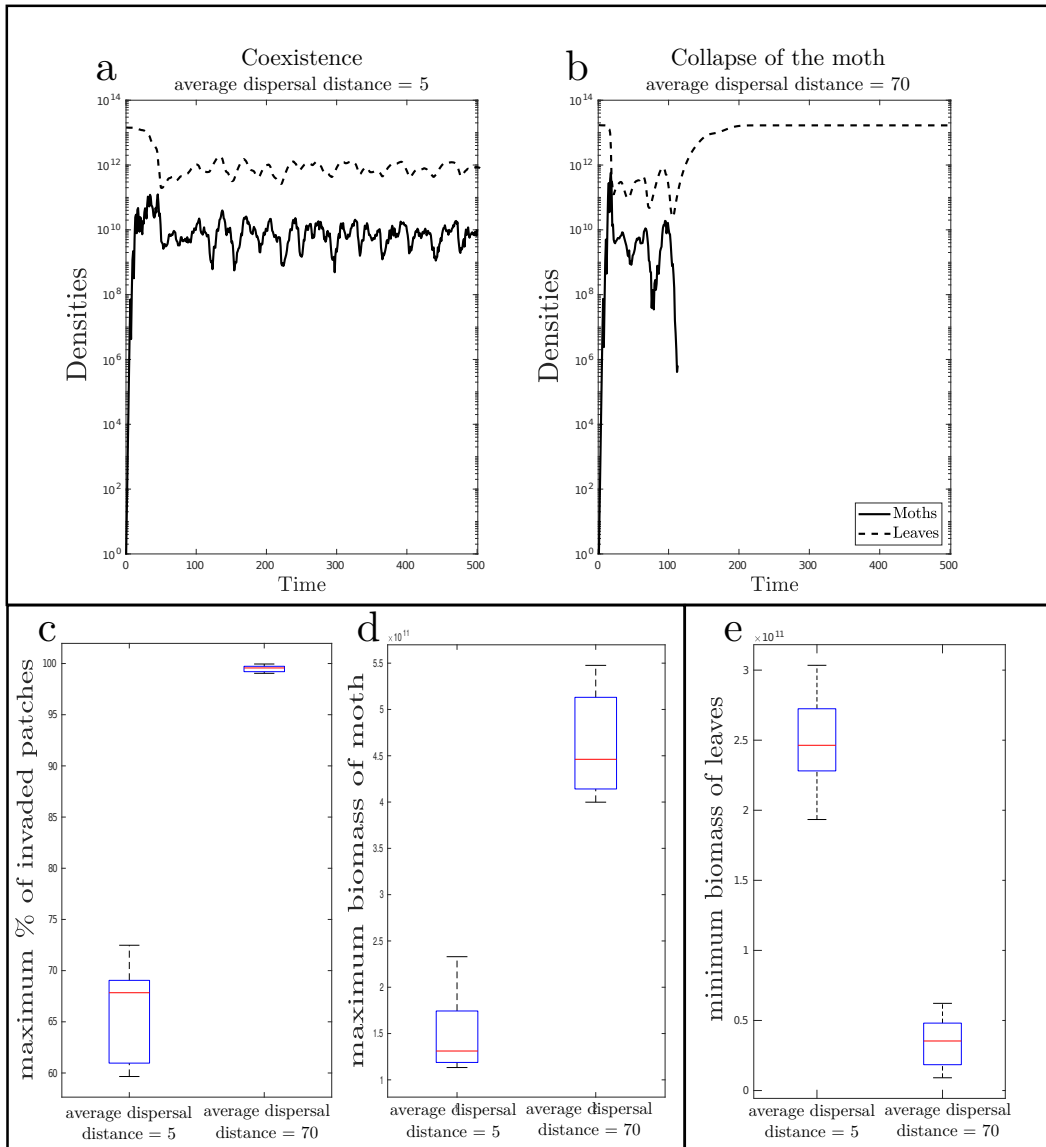


Figure 6

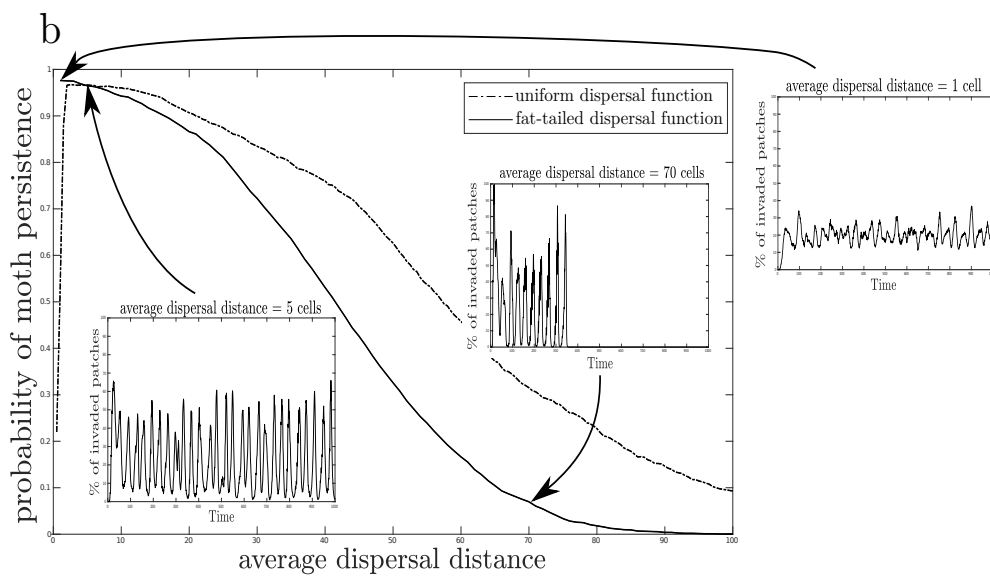
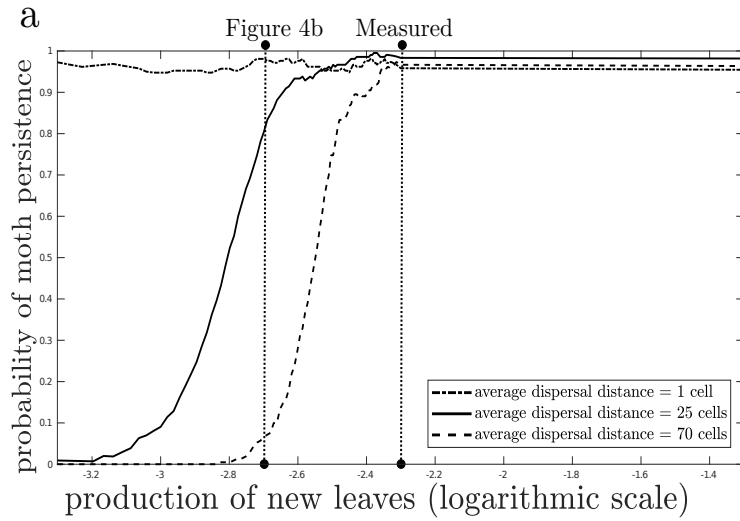


Figure 7

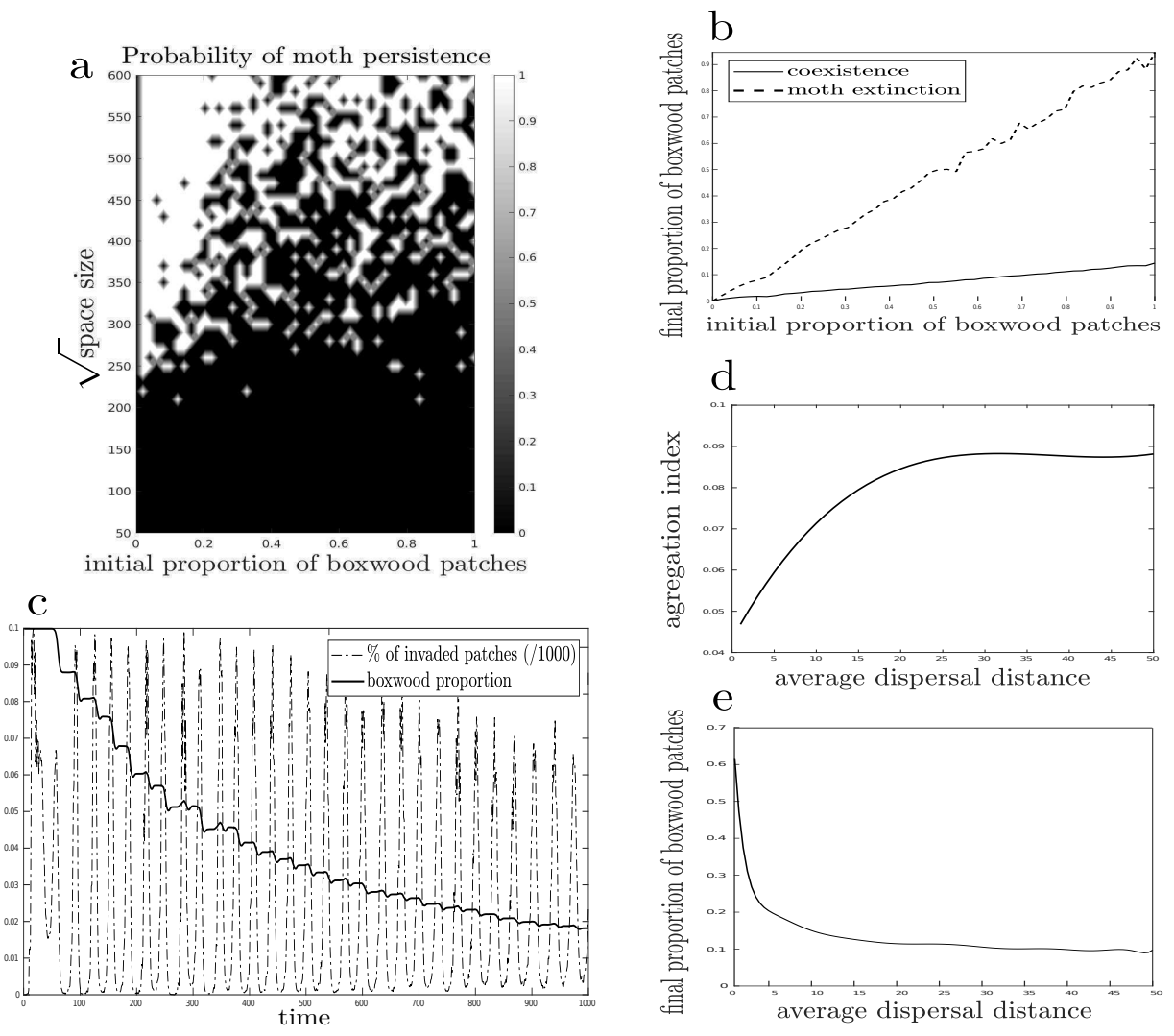


Figure 8

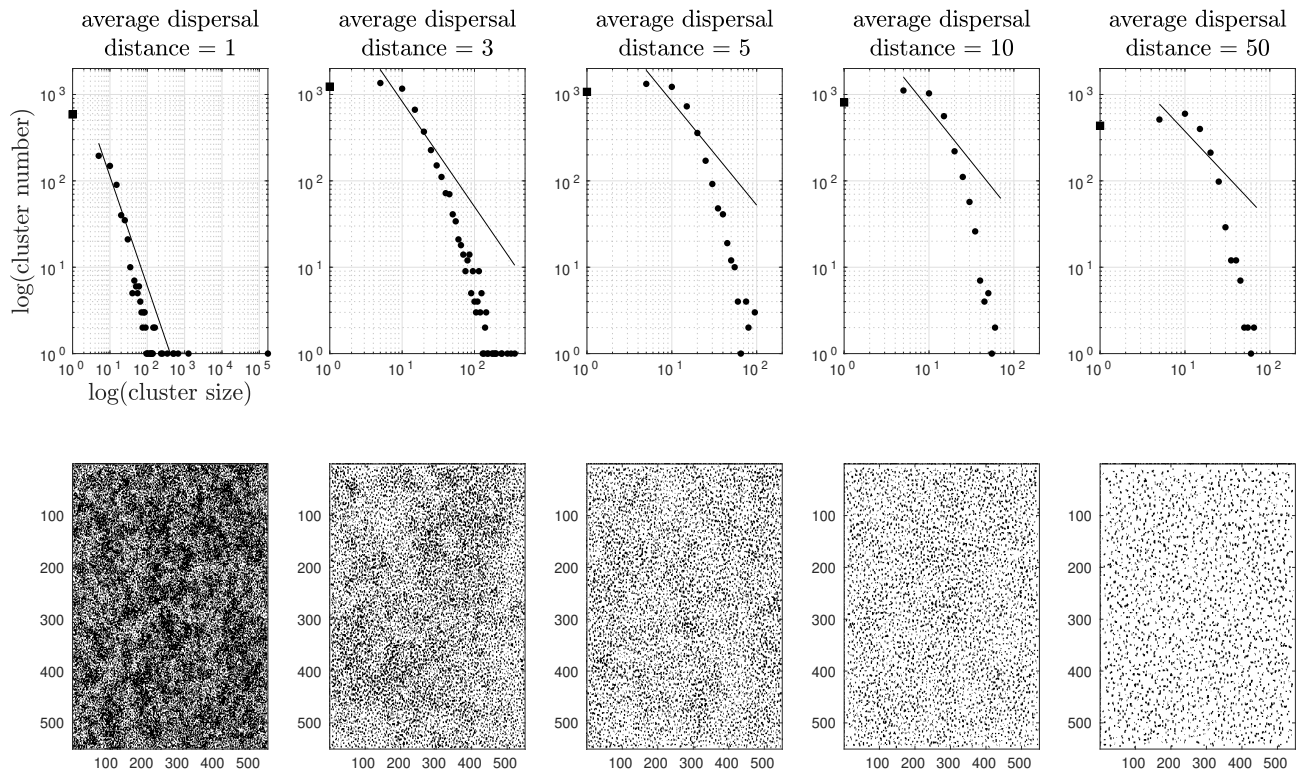


Figure 9